Institution: University of Strathclyde

Department: Biomedical Engineering

Title of Thesis: Three dimensional printing of complex anatomical structures for aid in planning cardiovascular paediatric surgery

Name of Author: Marc Boyce

Supervisors: Professor Terry Gourlay

Dr Monica Rozeik

Degree: MSc Biomedical Engineering

Year: 2015

‘This thesis is the result of the author’s original research. It has been composed by the author and has not been previously submitted for examination which has led to the award of a degree.’

Signed: Date:

Acknowledgment

I would first like to thank my family, for everything they have done to get me to this point in my life. There are some persons of note that made this project possible, firstly my supervisor Professor Terry Gourlay (one of the few cricket fans in Glasgow), Dr Monica Rozeik, who has been there for me providing guidance from day 1 of this project, I really appreciate it. Mr Mark Danton, the cardiac consultant surgeon who provided his appraisal of the model, and Dr Kasra Shaikhrezai for his clinical assistance.

Table of Content

Declaration of Authenticity 1

Acknowledgement 2

Abstract 5

1. Introduction

1.1 Normal Anatomy 6

1.2 Pathology Description 9

1.3 Method of Assessment

1.3.1. Echocardiography 10

1.3.2. Magnetic Resonance Imaging 12

1.3.3. Computerized Tomography 13

1.4. Limitations of Current Imaging Modalities 15

1.5 Surgical Techniques

1.5.1. End-to-end Anastomosis 16

1.5.2 Subclavian Flap Aortoplasty 18

1.5.3 Balloon Angioplasty 19

1.5.4 Prosthetic Patch 21

1.6 Cardiac Surgeons Need for Greater Planning 22

1.7 Rapid Prototyping 24

1.7.1. Liquid base RP 24

1.7.2. Solid base RP 24

1.7.3 Powder base RP 25

1.8 Rapid Prototyping as an Aid to Surgical Planning

1.8.1 Models, Surgical tools and Implants 26

1.8.2 Surgical Models for Training Purposes and Medical Devices 27

1.8.3 Scaffolds for Tissue Engineering 28

1.9 Medical Requirements of Rapid Prototyping 29

1.10 Limitations of Rapid Prototyping 30

2. Objectives 31

3. Methodology

3.1 Generating Computational 3D Anatomical Model 32

3.2 Computational Fluid Analysis 34

3.3 Printing Anatomical Structures 37

4. Results

4.1. Computational Fluid Dynamics 43

4.2. Printed Anatomical Model 45

5. Discussion

5.1. Computational Fluid Dynamics 46

5.2. Physical Model 47

5.3. Limitations 50

6. Conclusion 51

7. References 52

8. Appendix 1 59

Abstract

Congenital heart disease is a collection of defects present at birth which impact on the normal functions and anatomical structure of the heart. One such condition is coarctation of the aorta, a narrowing of the main blood vessel leading from the left ventricle, responsible for blood transport to the body. It is estimated to affect between 3000 and 5000 persons each year in the US. Surgeons have relied on conventional imaging modalities, primarily echocardiography, magnetic resonance imaging (MRI) and computed tomography (CT) for diagnostics and planning of the corrective surgery. These modalities have limitations, even though some 3D projections based on volume rendering can be generated using these modalities, one of the main limitations is they are two dimensional and are limited in perceiving depth. To reduce the impact of these limitations on surgeons planning surgery, use of computational fluid dynamics and liquid base rapid prototyping to produce 3D anatomical models of a coarcted aorta were employed. CT scans of a ten day old neonate were obtained, and using Mimics software a 3D computational model was generated from the images. The geometry was imported into Ansys fluid analysis software, generating a contour map of the wall shear stress and velocity vectors of blood flow through the aorta. The contour mapping showed elevated levels of shear stress at the point of coarctation, with a maximum shear stress of $2.7 \times 10^{-3}\ mmHg$ and a maximum blood velocity through the narrowed coarcted region of 6.97 m/s. The physical 3D model printed from the geometry was critically appraised by a consultant cardiac surgeon, his findings proved the model very useful in the aid of surgeons for the purpose of planning a corrective surgery. The model showed great detail and provided a comprehensive analysis of the legion not provided by current imaging modalities.

Three dimensional printing of complex anatomical structures for aid in planning cardiovascular paediatric surgery

1. Introduction

Congenital heart disease as the umbrella term covering a wide range of defects present at birth that affects the way the heart should normally function. The focus of this research will be on congenital heart disease and more specifically coarctation of the aorta, and how the physical modelling of this abnormality could provide a greater benefit to the surgeon in the planning of a corrective surgery. Early research of congenital heart disease, indicate low occurrences of about 4 to 5 for every 1,000 live births, but this has since risen to about 12 to 14 for every 1,000 live births, this figure may be higher yet in recent times (Hoffman and Kaplan, 2002). Coarctation of the aorta occurs in 8 to 11% of these congenital heart defects which is between 3,000 and 5,000 patients each year in the US (Ladisa, Taylor, and Feinstein 2010).

1.1 Normal Anatomy

The aorta is the main artery leading from the left ventricle of the heart and branches into a network of arteries that perfuse the body. The normal aortic structure includes an ascending segment called the ascending aorta, a transverse segment or curvature called the arch, and a descending segment called the descending aorta or abdominal aorta which divides to form other arteries which perfuse the lower body. The ascending aorta stretches from the left ventricle, starting with the aortic root which includes the aortic valve, annulus, and valvular sinuses to the base of the innominate artery, which branches to form the right subclavian as well as the left and right carotid arteries (see fig.1). The aortic arch extends from the innominate artery and terminates at the ligamentum (ductus arteriosum). The distal or most outer region of the arch, after the left subclavian artery is called the aortic isthmus. The aortic arch is most commonly found on the left side of the patient's body. The descending aorta starts at the ligamentum and branches into the intercostal arteries and bronchial arteries (Goo et al. 2003).

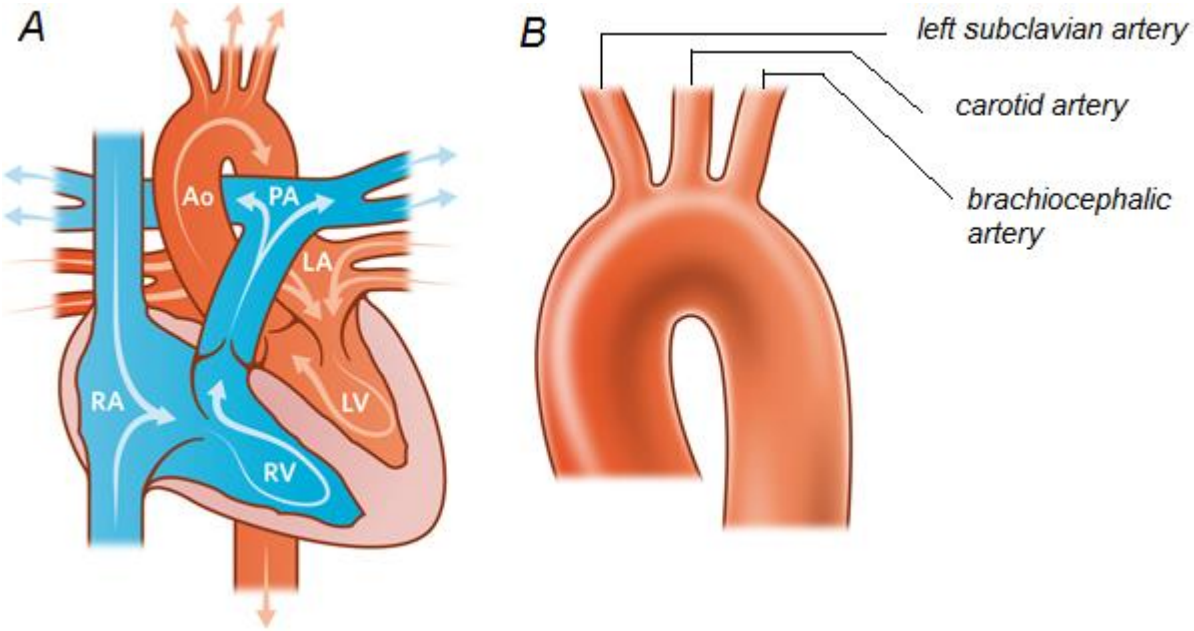

Fig. 1 (A) showing the normal circulation and anatomy of a healthy heart, arrows indicating direction of blood flow. RA labels the right atrium, RV the right ventricle, PA the pulmonary artery, LV left ventricle, LA left atrium and Ao the aorta. (B) showing a healthy aorta with uniform diameter throughout the entire length of the vessel. Image by (Melbourne 2015).

The main function of the circulatory system in both the foetus and the neonate is to facilitate gas exchange, and rid the body of waste products such as carbon dioxide while supplying the organs with oxygen and other nutrients. During the foetal stage, gas exchange takes place in the placenta, and it is connected in parallel with the arterial system to the other organs, and isolated from the pulmonary circulation. In order for gas exchange to take place, deoxygenated blood is delivered to the placenta and oxygenated blood returned to the arterial circulation, the placenta acts as the lungs in mature humans. To aid this process, the arterial and pulmonary circulations are connected by extracardiac shunts in the form of the ductus venosus and the ductus arteriosus as well as intracardiac in the form of the foramen ovale (see fig.2). After birth, gas exchange is relayed to the lungs, this moves dependency from the systemic arterial circulation to the pulmonary circulation. In a healthy neonate, the venous and arterial circulations are disconnected, the foetal shunts close to become ligaments, and their continued patency can lead to circulatory complications. The circulatory evolution from foetal to neonatal is defined by the discontinuity of the

arterial circulation to the placenta, the expansion of the lungs with air, the increase in blood flow to the lungs, and closure of ductus arteriosus and ductus venosus. If the foetal shunt pathways stay open after birth, can be seen in some congenital heart disease such as coarctation of the aorta, it causes a diversion of blood flow, allowing a mixture of oxygenated blood and deoxygenated blood. This ductal-dependent systemic circulation is not well tolerated and may lead to complications in the newborn, this is mainly because the normal closure of the ductus arteriosus reduces systemic blood flow. Ductal-dependent pulmonary circulation may also result in severe reduction in the levels of pulmonary blood flow (Friedman and Fahey 1993).

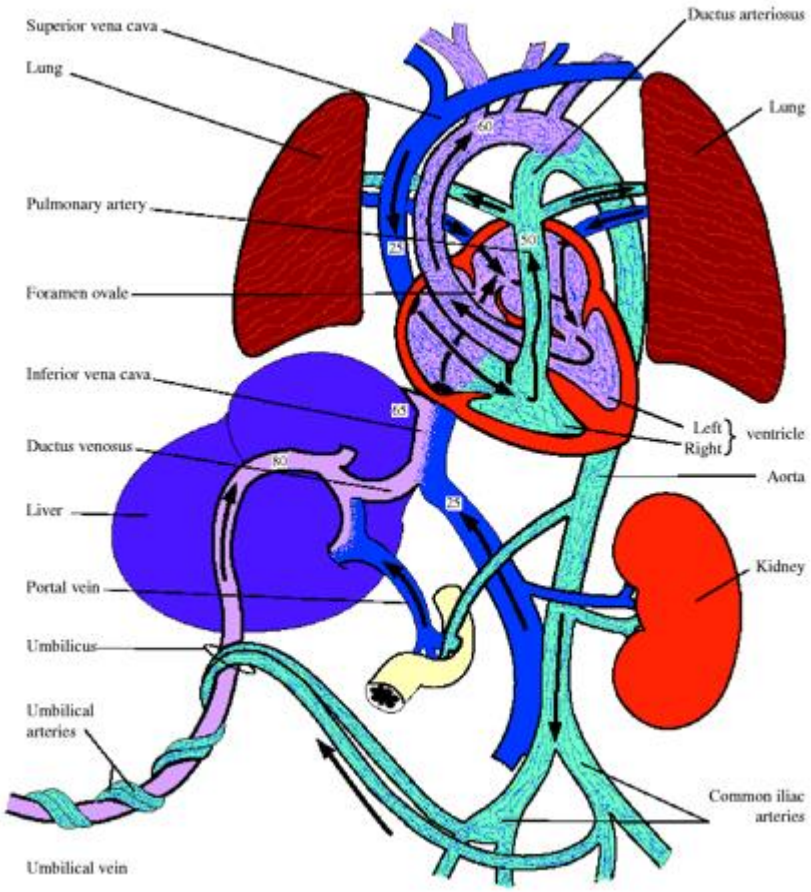

Fig. 2 showing the structure of the circulatory system of a human fetus, the before described foetal shunt pathways (ductus venosus, ductus arteriosus and foramen ovale) can be seen on this diagram. Image by (Murphy 2005).

1.2 Pathology Description

Coarctation of the aorta (CoA) is a congenital heart disease that presents as a narrowed or constricted section of the main artery called the aorta (see fig.3). The malformed section of the vessel involves all layers of the wall, inclusive of the anterior, superior and posterior layers of the wall, it may be a short discrete section or an elongated narrowing. The lesion may occur at any point on the aorta, however it is most commonly found opposite the ductus or before the ductus (preductus) in infants and at the ligamentum arteriosum in adults or adolescents. In isolated cases, the deformity may be found in the abdominal aorta or above the left common carotid arteries along the arch (Fuster et al, 2011).

CoA rarely occurs as a single defect, it is usually accompanied by other defects such as tubular hypoplasia of the aortic arch, aortic stenosis or bicuspid aortic valve. It is common for the clinical symptoms of coarctation to be presented as hypertension of the upper body, superior to the narrowing and hypotension of the lower body, inferior to the constricted area. Heart failure is also presented in most cases within the first two months of life for neonates born with this defect. Common clinical characteristics of CoA are cardiac murmur and a blood pressure gradient during systole between the upper and lower body of >10 mm Hg. Pulses in the lower body are reduced in 74% and completely absent in 18% of patients, 94% show signs of upper-extremity hypertension and 50% have systolic blood pressure >140 mm Hg (Ing et al. 1996).

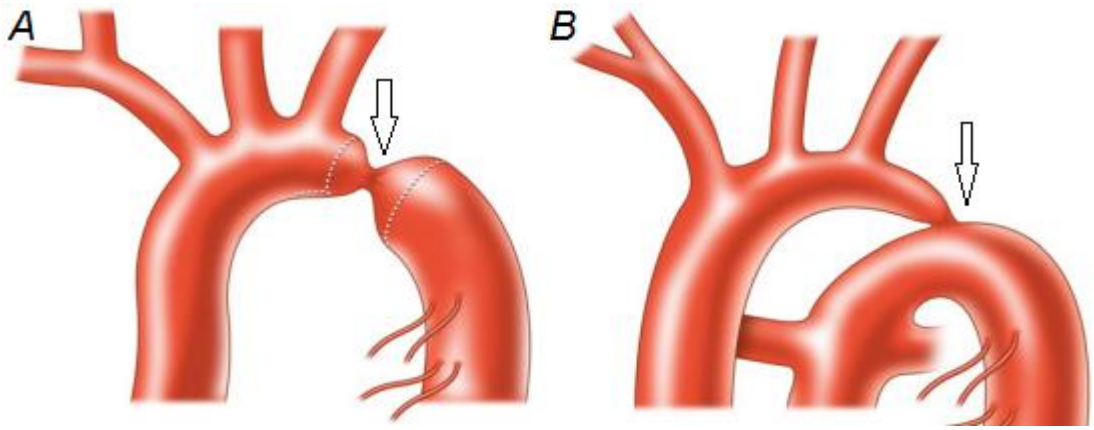

Fig 3. (A) Showing a discrete coarctation indicated by an arrow, the narrowing presents as a sharp reduction in diameter of the vessel. (B) Shows coarctation accompanied by arch hypoplasia, there is a discrete narrowing but also an elongated reduction in diameter spanning a portion of the arch. Image by (M. Lee, d'Udekem, and Brizard 2014).

1.3 Methods of Assessment

Currently surgeons rely predominantly on imaging modalities for the assessment and subsequent preparatory planning for cardiac surgery to repair severe coarctation of the aorta. The definitive diagnosis or datum standard of congenital heart disease has been cardiac catheterization and angiocardiography. These procedures are risky, even more so in the severely ill neonates, hence non-invasive methods have been the preferred alternative (Meyer and Kaplan 1973). Methods such as:

1.3.1 Echocardiography

Echocardiography is the first investigative step into congenital heart disease. It is a non-invasive imaging tool which allows for the real time monitoring of cardiac structures with the use of ultrasound for the purpose of inspection and evaluation (see fig.5). It is used by paediatric cardiologist at the foetal stage, or in neonates (Sahn et al. 1975). Doppler gradients and the absence or reduction in pulses of flow may also be detected. The use of Doppler ultrasound imaging techniques allows the inspection of foetal anatomy with fine detail, this can be done as early as 14-16 weeks gestation to identify structural and functional abnormalities of cardiac anatomy

(Macartney, 1986). Foetal echocardiography have been used in the detection and diagnosis of congenital heart disease prenatally with some degree of success. Prenatal diagnosis of coarctation, though more difficult than originally thought, can be done using this technique. In a study of 78 suspected cases of coarctation using this method, 50 cases were confirmed after the birth of the child (Sharland, Chan, and Allan 1994). Echocardiographic examinations are commonly performed from the position of the suprasternal notch, this technique is used to image the transverse aorta, right pulmonary artery and left atrium (see fig.4). It has proven useful for the analysis of congenital heart disease including coarctation of the aorta (Snider and Silverman 1981).

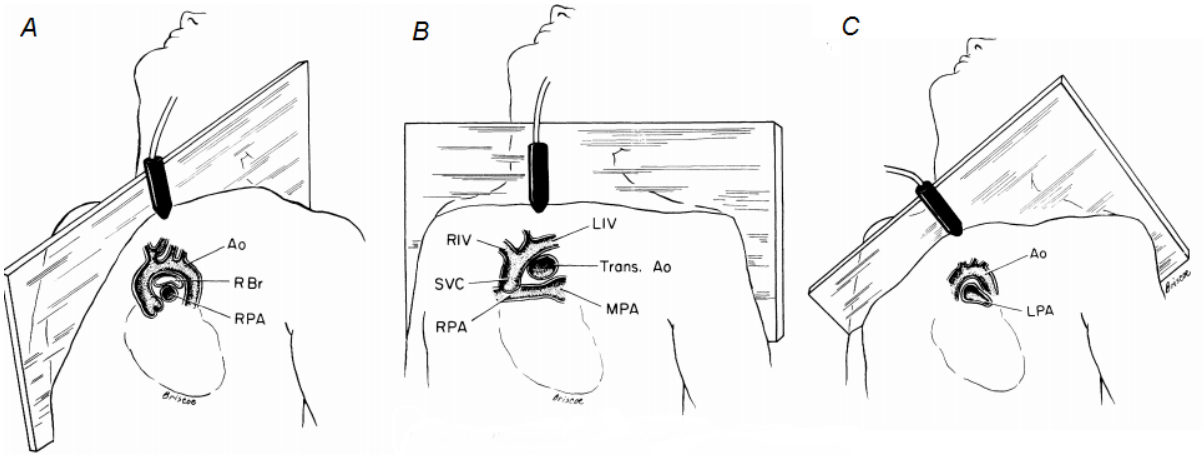

Fig 4. showing the position of the transducer for the different planes of the suprasternal view. (A) show the long axis suprasternal notch view. It establishes a diagonal plane passing through the chest between the right breast and the left scapular tip. Clearly visible on this plane is the ascending, transverse and descending aorta (Ao), the right pulmonary artery (RPA) and right mainstem bronchus (RBr). (B) shows the short-axis view used to image a cross sectional view of the transverse aorta (Trans. Ao), the right pulmonary artery (RPA), the right and left innominate veins (RIV and LIV), superior vena cava (SVC) and the main pulmonary artery (MPA) in the coronal (frontal) plane. (C) shows the long-axis plane used to image the left pulmonary artery (LPA). Image adapted from (Snider and Silverman 1981).

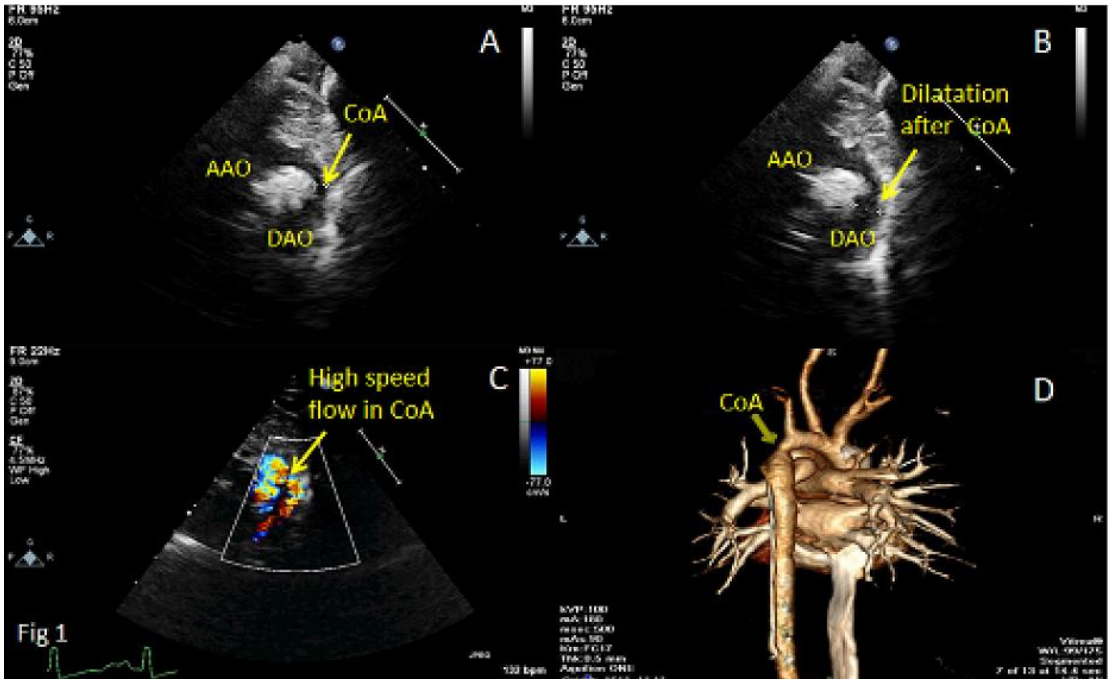

Fig 5. shows a transthoracic echocardiogram taken at a suprasternal view. (A) Shows the area of coarctation (CoA) as well as the ascending (AAO) and descending aorta (DAO). (B) Shows the area after coarctation where the aorta becomes wide again. (C) Shows the abilities of Doppler ultrasound to image and colour code the velocity of blood at different regions of the anatomy. (D) Shows a 3D verification of the coarctation of the aorta with the use of computed tomographic angiography. Image by (Sun et al. 2015).

1.3.2 Magnetic Resonance Imaging (MRI)

MRI is an excellent non-invasive imaging modality for imaging congenital defects of the major arteries in paediatric patients and may provide additional information regarding the defect. MRI is known to provide details of lesions that echocardiography either failed to provide or proved inconclusive, including coarctation of the aorta (Fletcher and Jacobstein 1986). Electrocardiographically gated MRI is known to be successful and produce high resolution diagnostic images, clearly depicting the position and shape of the narrowed section. It also shows the relation of the narrowing to surrounding anatomy such as arteries branching from the aortic arch and to the aortic isthmus and the distal aortic arch (see fig.6 &7). MRI produced images which captured the anatomy better than any other non-invasive technique. It provided most of the anatomical information required to perform the corrective surgical procedures (Baker et al. 1989).

Fig 6. showing a MR angiogram with the use of contrast agent. Image by (Allen et al. 2013).

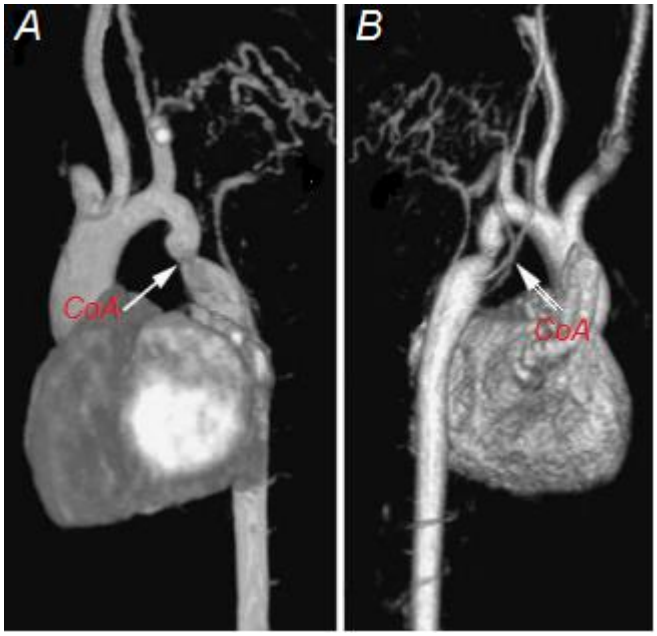

Fig 7. (A) Showing volume rendering (2D projection of 3D data comprising of many slices) and (B) 3D reconstruction, of contrast enhanced MRA imaging with the area of coarctation indicated by arrows. Image by (Didier et al.)

1.3.3 Computerized Tomography (CT)

Multi-slice spiral CT has improved the clinical relevance of cardiac CT imaging in patients with congenital heart disease. Allowing for the capture of volume data along

with fast scan speeds and quality spatial resolution, it improves the ability to clinically analyse structural abnormalities and defects in patients with congenital heart disease (see fig.8). It can also be combined with ECG gating, to provide information on ventricular wall motion, ventricular ejection, and valvular motion, as well as coronary CT angiography (Goo et al.). A study of 14 patients comparing axial, multiplanar, and 3D volume-rendering imaging was described. The results indicated accuracies ≥ 96% for diagnoses of aortic position and narrowing on all image types. The diagnosis of coarctation, were 73% for axial, 100% for multiplanar, and 100% for 3D volume-rendered images. There were no significant statistical differences in diagnostic performances between the imaging techniques ($p > 0.05$). Axial, multiplanar, and 3D volume-rendered images performed equally well in assessing the aorta from a side view to diagnosis. Multiplanar and 3D volume-rendered images perform slightly better compared to axial images in the evaluation of coarctation of the aorta (E. Y. Lee et al. 2012).

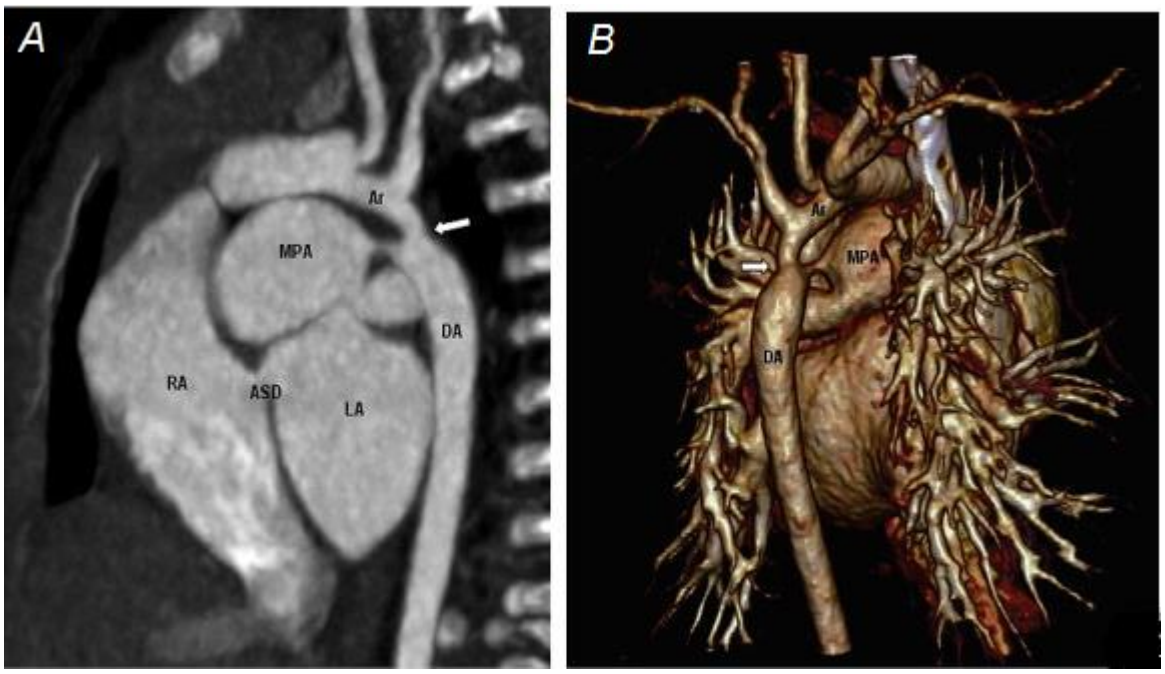

Fig 8. shows a Computed tomographic image, from the image the area of coarctation is identified with an arrow, other anatomical landmarks include left and right atrium (LA and RA respectively), an atrial septal defect (ASD) which is a whole in the septal of the heart (the wall separating the left and right atriums), the aortic arc (Ar), descending aorta (DA) and the main pulmonary artery (MPA). (A) Shows the image of one slice from the CT scan, (B) shows the 3D reconstruction, clearly indicating the region of coarctation. Image by (Nie et al. 2012).

1.4 Limitations of Current Imaging Modalities

Echocardiography (echo) and conventional angiography have long been the main methods of evaluating congenital heart disease, however, they both have limitations. Echocardiography identifies and defines intracardiac anomalies and estimates the haemodynamics very well. Its limitations arise from a small field of view, a variable acoustic window, an inability to adequately infiltrate air and bone, and an inefficiency to precisely differentiate extracardiac structures (Haramati et al. 2002). Echo proved to be operator dependent and may sometimes be insufficient for thoroughly evaluating complex anatomical structures such as the coronary arteries, the aorta and branches of the pulmonary artery and veins. It is also susceptible to motion artefact caused by patient breathing and heartbeat. Angiography, an invasive procedure requiring catheterization, runs the risk of vessel damage, hemorrhaging, stroke and infection. Another drawback is it produces 2D images which may not provide the surgeon with the true extent of the problem at hand, particularly in neonates with tiny complex anatomies. Multidetector CT technology has improved speed, and with ECG-gated acquisitions reduces error due to motion artefacts caused by respiration and cardiac movement. This can greatly improve visualization of the anatomy of the heart in neonates (Ben Saad et al. 2009). CT provides a faster method of imaging with high spatial resolution however, it does not provide functional information such as ejection fraction and regurgitation fraction which are important in surgical management and can be obtained by MRI or Echo (Goo et al. 2003).

Surgery is usually performed on the basis of clinical data and echocardiographic images without the use of MRI or CT. In patients with characteristic symptoms based on clinical or echocardiographic analysis, there has been an adjustment or change to the plan for treatment after additional information had been discovered following CT and MRI. An experiment was described where MRI and CT were used to evaluate four patients suspected of having coarctation of the aorta but had a failed diagnosis using echo, it failed to provide sufficient detail to confirm or dismiss the claims. The final diagnosis was patient specific, but it required the use of more than one modality to successfully portray the coarctation of the aorta. A follow up of two of the patients

who had received balloon angioplasty as the treatment for their condition, required additional MRI to supplement echocardiography. MRI and CT fills a void created by the limitations of echocardiography and angiography, especially when it comes to defining extracardiac arterial anatomy in patients with congenital heart disease (Haramati et al. 2002). CT also comes with its limitations, a study aimed to compare the accuracy of three-dimensional geometry of surface models reconstructed with either five Cone Beam CT scanners or one Multi-Slice CT was described. The accuracy of CBCT surface model was lower but still deemed acceptable in comparison to MSCT in relation to the gold standard. For MSCT, the mean deviation from the gold standard was 0.137 mm and for the five CBCTs were 0.282, 0.225, 0.165, 0.386 and 0.206 mm respectively (Liang et al. 2010).

1.5 Surgical Techniques

Surgeons and clinicians rely on various surgical procedures and techniques to correct congenital heart defects in infants and neonates, the majority of patients with a complex congenital heart disease will at some point undergo a single or combination of interventional, surgical and joint or hybrid surgical procedures (Bentham and Thomson 2015). The surgical operative approaches used to repair coarctation of the aorta are end-to-end anastomosis, prosthetic patch, subclavian flap aortoplasty, and prosthetic interposition or bypass grafts (Sweeney et al. 1985). Apart from surgical procedures there is the alternative of percutaneous balloon angioplasty (Rao et al. 1988). In more recent times this technique has evolved and may be done with or without the addition of a stent to prevent narrowing of the artery after the procedure (Harrison 2001).

1.5.1 End-to end Anastomosis

End to end is simply the removal of the narrowed section of the aorta, or coarcted region and joining the remaining portions of the vessel together at the two ends (see fig.9). This method of repair for coarctation is done through a serratus sparing left posterolateral thoracotomy gaining access between the 3rd or 4th intercostal space.

The lung is shifted anteriorly, and single lung ventilation is not induced. To gain access, an incision is made to the pleura above the narrowed section of the aorta, ensuring the preservation of the vagus and phrenic nerves is crucial. The incision in the pleural is expanded from the position of the left subclavian to midway in the descending aorta. This allows accessibility of the aorta from the distal end of the ascending aorta to midway in the descending aorta. If the patient is very young, distal circulation is dependent on the ductus arteriosus, division of the ductus or ligamentum, depending on the age of the patient will allow mobility of the aorta. Once these steps are successfully completed, anastomosis of the descending aorta to the inferior side of the arch can be freely undertaken. The aorta is clamped below the left carotid artery, this maximizes access to the underside of the arch while maintaining perfusion to the artery. The aorta is not perforated distal to the coarctation. The section of the aorta from the left subclavian artery to any normal area of the descending aorta, inclusive of the coarcted region is removed. The proximal end of the aorta immediately below the left carotid artery is attached either by sutures or staples to the distal end of the aorta. The patient's circulation is gradually restored. A sternotomy is performed for patients in need of a more proximal repair of arch hypoplasia (Wright et al. 2005). Problems may arise if the coarcted region is extended or if there is a mismatch in diameter of the two ends to be joined (Moor, Ionescu, and Ross 1972). During 1991 through 2007, a study of 201 patients who had undergone extended end-to-end anastomosis to repair coarctation of the aorta showed left thoracotomy was the surgical approach used in 78% and median sternotomy in 22% of the patients with a mean age of 23 days. Early mortality occurred in 2%. A follow up of 91% of patients after 5 $\pm$ 4.3 years showed recurrence of narrowing in 4.0%, of which 75% occurred in the first year after the operation (Kaushal et al. 2009).

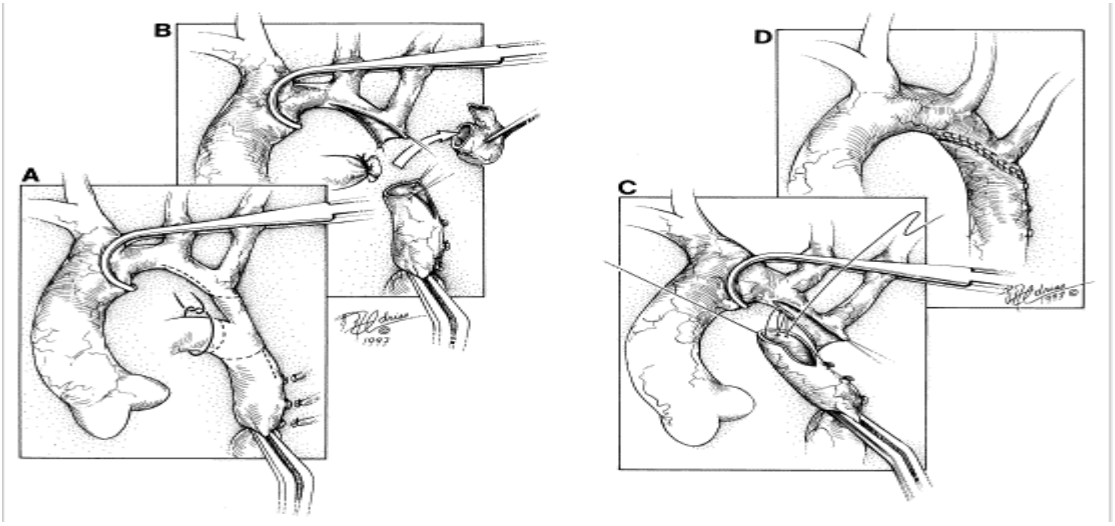

Fig 9. showing the end to end repair of coarctation of the aorta, (A) shows the resected area outlined by dotted lines indicating there the vessel will be cut. (B) Shows the coarcted region being removed, the duct is severed and sutured shut. (C) Shows the two ends being sutured together, notice the ends are not flush but are diagonal. In some cases the ends are straight instead of diagonal. (D) Shows the completed operation, the diameter is now more uniform across the vessel. Image by (Carl L Backer et al. 1998).

1.5.2. Subclavian Flap Aortoplasty

This procedure repositions the left subclavian artery from the point of origin to its first branches. The left subclavian artery is detached from the aorta at its origin and is dissected along its length. The wall of the aorta is also dissected on the anterior side from the origin of the left subclavian artery to the descending aorta, approximately 12 to 15 mm after the narrowed region. The narrowed region is dissected along its length and opened. The left subclavian artery now forms a flap, this flap is sutured to the edges of the now open aorta, resulting in a wider surface area and diameter of the previously narrowed region. This technique attempts to preserve the blood flow to the left arm (see fig.10). A follow up study of four patients pertaining to the technique postoperatively showed sufficient correction and suggested normal growth rate of the vessel at the site of coarctation. The study also indicated that the blood flow through the left subclavian artery was preserved, this was confirmed by Doppler measurements showing normal blood flow to the left arm without a pressure gradient. This technique is recommended in most cases of discrete coarctation and in some cases with an extended narrowing of the isthmus for patients of a range of ages and weights (Meier et al. 1986). In a study conducted

between January 1984 and December 2004, involving 119 infants who underwent isolated subclavian flap repair for coarctation, the mortality prior to hospital discharge was 4% and the late mortality after hospital discharge was 6%. Survival rates after 1 year was 91%, after 5 years was 85%, and 10 years after surgery was 85%. The rate of restenosis or renarrowing of the vessel was 11%. (Barreiro et al. 2007).

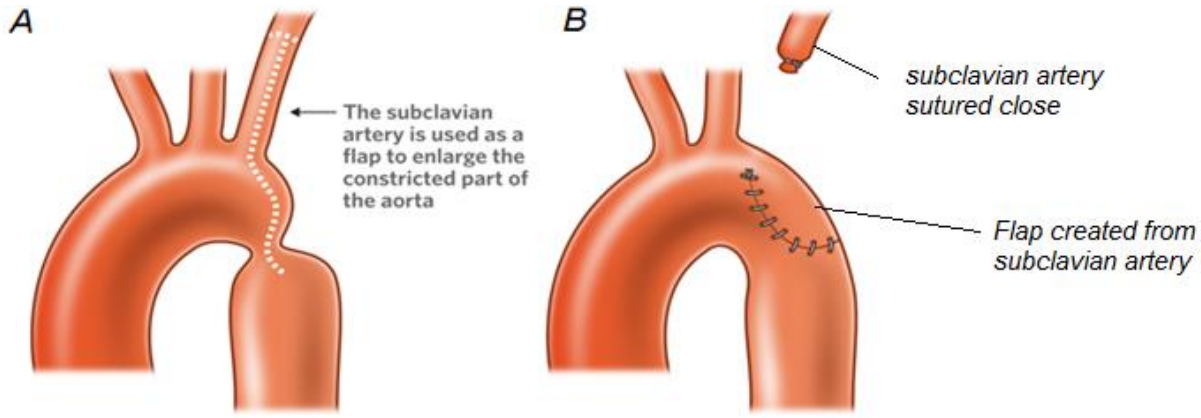

Fig 10. showing how the subclavian artery is sacrificed and used as a flap to expand the diameter of the aorta at the site of narrowing. Image adapted from (Melbourne 2015).

1.5.3. Balloon Angioplasty

Balloon angioplasty involves the deployment of a balloon catheter to the area of coarctation, the inflation of the balloon expands the narrowed section of the aorta (see fig.11). Stenting takes this a step further, a crimped stent is placed over the balloon, and upon inflation the stent is expanded and holds the vessel in a dilated positon. Therapeutic cardiac catheterization is done under anaesthesia, the coarctation is accessed retrograde, and a coronary wire is used for recordings of the gradient across the coarctation whenever necessary through the course of the procedure. A series of angiographic images of the aorta are obtained for references to anatomical landmarks to ensure precise placement of the stent. Some commonly used landmarks are the ribs and the tip of the venous catheter placed in the pulmonary artery. Preplacement expansion of the vessel with a balloon catheter is frequently performed, followed by catheterisation to determine the new pressure

gradient. The stent after being crimped onto a balloon catheter is navigated to the narrowed segment, this system and technique is designed to limit haemorrhaging and stent migration during introduction to the aorta. Positioning the stent is very important, precision is key in placement at the specific location prior to balloon expansion, considering also the shortening of the device when expanded. The size of the balloon must vary in patients to accommodate the difference in diameter of the aorta. A balloon size of approximately 7 mm is used for the neonates and infants, while a 10 mm balloon is used for the adolescents and adults. (Suárez de Lezo et al. 1995). A study to compare results of expansion of coarctation of the aorta with and without stenting was described. Patients who had undergone balloon angioplasty alone were group 1 and those with stenting were group 2. A reduction in the peak systolic pressure gradient was recorded in group 1 from 63.3 (22.8) to 10.7 (10.8) mm Hg, $p < 0.001$ and group 2 from 63.9 (20.8) to 2.7 (4.3) mm Hg, $p < 0.001$, a greater change is recorded in group 2. A pressure gradient of > 10 mm Hg indicates the group most at risk of developing further complications. The employment of multivariate Cox regression analysis, suggested the presence of a residual gradient as the main indicator to risk of developing further complications. The type of coarctation legion and the use of stent contribute to the presence of a residual gradient, and are common factors in producing a gradient of ≤ 10 mm Hg. Therefore the target of percutaneous treatment for coarctation should be to obtain gradients under 10 mm Hg, either by balloon angioplasty alone or with the implantation of a stent. It is recommended patients with hypoplastic isthmus or tubular coarctation should have stenting to achieve this reduction in gradient (Zabal 2003).

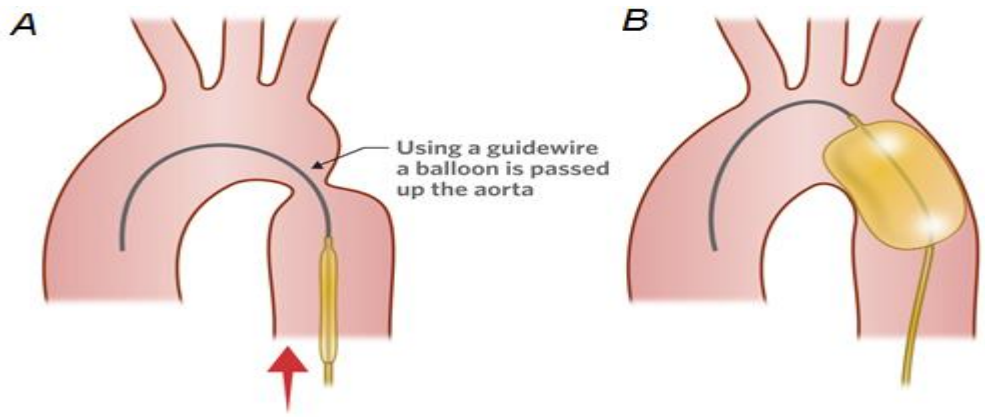

Fig 11. illustrates the principal of balloon angioplasty, (A) shows the deflated being transported along a guide wire to the point of coarctation. (B) shows the inflated balloon in position. Image by (Melbourne 2015).

1.5.4. Prosthetic Patch

This procedure is performed through a left lateral thoracotomy through the bed of the fifth rib. The mediastinal pleura is incised, and the left subclavian artery and the aorta are taped proximal and distal to the narrowed region. The intercostal vessels are clamped and ligated, sometimes it may be possible for them not to be exposed. After the major vessels are secured by clamping, a longitudinal slit is made in the aorta from a point distal to the narrowed region, transverse the isthmus and finishing at a proximal region. If lumen is completely occluded, this may still be possible. The diaphragm is excised. Dacron is usually the material of choice for the patch, though sometimes other materials such as arterial tissue can be used to produce an autograft. The shape and size of the material is patient specific, the patch is usually adjusted during the operation. The patch is sutured in place, creating a wider diameter of the aorta in the area of the coarctation (Moor, Ionescu, and Ross 1972). The risk of developing an aortic aneurysm subsequent to coarctation repair with a prosthetic patch is very likely and can be life threatening. The use of synthetic materials such as Dacron® increase the risk of aneurysm formation and possible rupture. A study seeking to investigate the occurrences of aneurysm in patients who have had coarctation repair with the use of a Dacron® patch was conducted between 1977 and 1994. A total 63 patients had the repair using the patch. Aneurysms were determined based on an aortic diameter of at least 1.5 times that of the diameter of the aorta at the level of the diaphragm as imaged by angiography, CT, or MRI. The

results showed 47 % developed an aneurysm at the site of repair, 31% of those aneurysms ruptured resulting in death in 77% of the patients who experienced a rupture. After five years, 97% of patients had yet to develop an aneurysm, after ten years 90%, after 20 years 69%, and 42% after 25 years. It was determined the risk of developing an aneurysm at the site of repair and subsequent rupture resulting in death is extremely high for this particular material (Cramer et al. 2013). Therefore in 2008 the American Heart Association/American College of Cardiology (AHA/ACC) guidelines stated all patients who had repair for coarctation of the aorta with a Dacron® patch should have a CT or MRI done at least every 5 years for screening of possible aortic aneurysm formation (Warnes et al. 2008; Cramer et al. 2013).

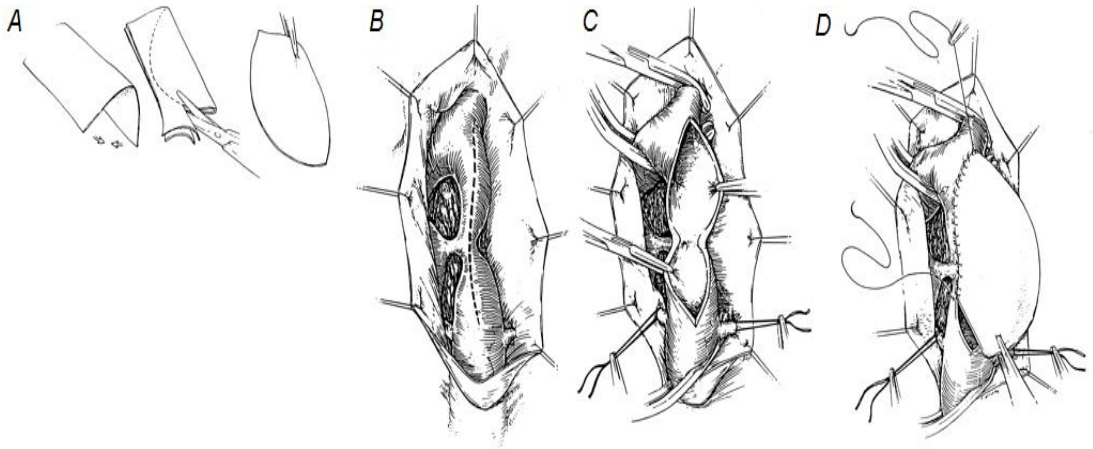

Fig 12. shows the steps in performing patch repair for coarctaion of the aorta. (A) shows the preparation of the material, Dacron is most commonly used. (B) shows the narrowed section of the vessel and the duct connecting the pulmonary artery, the dotted line represents the path for surgical incision into the vessel. (C) shows the vessel after incision and (B) shows the patch being sutured into position creating a wider diameter of the aorta. Image by (C. L. Backer et al. 1995).

1.6. Cardiac Surgeon's Need for Greater Planning

Cardiac surgeons have long acknowledged the need for a study which links human factors to the outcome of surgery, particular in paediatric cardiac surgery as it is a complex field and has a low margin for error. It includes various complex procedures that are not only highly dependent upon an intricate organizational structure, coordinated team efforts of a strategic multidisciplinary unit, and high levels of

cognitive and technical ability, but also on the planning of the surgery. Patient groups such as neonates and infants are considered high risk, because of a very fragile anatomy and tiny frame. Advances in technology and surgical techniques have allowed for greater performances and an increase in favourable outcomes in the early completion of surgical repairs. These repairs are often done in neonates and infants within the first couple years of life. At this stage of life, the complexity of the procedure is greatly increased, the internal anatomy is in much closer proximity to each other and the patient is not fully developed

A study interviewing surgeons from three teaching hospitals revealed that of 146 incidents, 33% caused permanent disability to the patient, 77% of these occurred during an invasive or surgical procedure, and 66% occurred in the intraoperative phase in theatre, the data of the study focuses primarily on this period during surgery (Gawande et al. 2003). Several factors have been linked to the poor outcomes in paediatric cardiac surgery, including institution, unique limitations of the surgeon, complexity of case, and systems failures. The bulk of the incidences reported were system factors, mainly as the result of the inexperience of the surgeon or lack of competence in performing the specific surgical procedure. Other reasons for adverse results during surgery included miscommunication among surgical personnel, fatigue or excessive workload placed on the surgeon, and immediate emergency surgical care (Galvan et al. 2005). For deaths during paediatric cardiac surgery that were deemed avoidable as described by The Bristol Royal Infirmary Inquiry and the Manitoba Inquiry, have both suggested that they identify the impact of human factors and systems research in paediatric cardiac surgical outcome(Sinclair and Court 2000; Galvan et al. 2005).

The overall mortality rate for all operations repairing congenital heart disease on children older than 1 year is 4%. Mortality rates for the surgical repair of coarctation of the aorta specifically is 1.1% (Stark et al. 2000). The mortality rates of repairs in neonates are in the range of 10–40%, depending on the category, which is based on severity of the deformity, and the type of repair procedure performed (Jenkins et al. 2002).

In an effort to better prepare surgeons for surgery, the creation of virtual and physical three dimensional models to better visualize the anatomy was employed. These models also provided an aid for the surgeons to practice the procedure before performing the actual operation on a live patient where the margin for error is very small. A technique called Rapid Prototyping was adapted to this field to manufacture the models.

1.7. Rapid Prototyping

There are numerous ways to produce RP models, however they all can be categorized based on the state of the build material as either liquid base, solid base or powder base prototyping systems.

1.7.1. Liquid base RP

This technique uses an organic photocurable resin which solidifies when exposed to UV rays. It cures the resin one layer at a time until a fully formed art is completed, this is done in a vat, a very large tank. An example of this is 3D Systems Stereolithography apparatus (SLA), it produces a 3D object from liquid photosensitive polymer resins which polymerise at the surface when introduced to UV light in the form of a laser. The laser is manoeuvred over the surface of the liquid causing it to solidify, when this layer is complete it is lowered into the resin allowing for a new layer to be added to it, this process is repeated until the part is formed (Noorani 2006; Chua, Leong, and Lim 2010).

1.7.2. Solid base RP

This technique involves numerous different methods in producing 3D models from solids in various forms, these forms are however separate from powders. One example of this is Solidscape's 3D printing and deposition milling. This technology utilizes dual ink printer heads to apply a thermoplastic material and a wax support

simultaneously, these materials are applied in thin layers building up to form the finished object. This method has been applied across numerous fields to produce everything from jet engine turbine blades to jewellery (Noorani 2006; Chua, Leong, and Lim 2010).

1.7.3. Powder base RP

This technique uses powder as the build medium, the methods are similar to those utilised for liquid base RP with the use of light I the form of laser to solidify the material. However, there are also techniques which 3D print from a base material that is powder, these methods are similar to solid base RP. An example of this is the 3D systems' selective laser sintering (SLS), where a CO_2 laser traces the object layer by layer in the powder, the heat generated from the laser sinters the powder causing it to bond. After every layer is sintered, a fresh layer of powder is added and the process is repeated until the complete object is formed (Noorani 2006; Chua, Leong, and Lim 2010).

1.8. Rapid Prototyping as an Aid to Surgical Planning

Since the development of Rapid Prototyping technology in the 1980s, it has enabled the production of prototypes which form actual models. Rapid prototyping (RP) has been successfully applied to the medical field. The RP creates a physical 3D model of a real life structure, in medicine it have been used to recreate parts of the anatomy. The 3D model produced can be utilised to improve the interpretation of a problem, provide further visual and physical analysis, and provide an additional tool for planning and practicing of a surgical technique before the actual operation in a pressure situation in theatre. RP involves the transformation of CT images to a physical 3D model, it is capable of producing models with great complexity in design with intricate detail. The model can be created within a short space of time of receiving the blueprint, it is these properties that creates possibilities for the use in the field of medicine. Mimics and software like it have helped to further develop RP, by allowing for the near precise replication of anatomy while providing the ability to segment specific structures. The software takes CT images and converts them to .STL

(Stereolithography) format, which is the standard file format for RP worldwide. The creation of life size models allows for simulations of the surgical procedure to optimize technique as well as measurement assessment for production of a prosthesis (Kai et al. 1998).

The three main applications of rapid prototyping in medicine are:

i.) Production and design of biological models, surgical tools and implants
ii.) Modelling for surgical planning and training, and medical devices
iii.) Production and design of scaffolds for tissue engineering

1.8.1. Models, surgical tools and implants

The production of physical models representative of anatomical structures created from 3D images. The use of this technology affords surgeons and medical doctors the luxury of an accurate replica of specific anatomical structures that may be used as an additional aid to the conventional imaging modalities for preoperative planning, diagnosis and treatment. These models have been successfully applied across various medical fields such as craniomaxillofacial, orthopaedic and dental surgery. The advantages of using such modelling include: region specific visualization and analysis; improved portrayal of information at the planning stage among all persons of interest that is the surgical team, radiologists, MD and patients; allows for the surgeons to rehearse their technique improving surgical time, as well as accuracy and safety of the procedure; the fabrication of patient specific implants for patients with complex defects, this eliminates prosthesis mismatch which sometimes occur with standard one size fit all prosthesis. This technique also proves very useful in cosmetic surgery (Kai et al. 1998; Corney and Hieu 2005)

Case study

A 20-month-old girl has a double outlet right ventricle was analysed for pending a possible biventricular corrective surgery. The patient had banding of the pulmonary trunk and surgical repair of coarctation of the aorta as a neonate. The flow out of the

left ventricle was partially blocked by infundibular musculature. Since both ventricles were well developed, the preferred surgical procedure was to create a baffle to reroute blood from the left ventricle to the aorta. The exact nature of the obstruction and the correlation of the outflow tract of the left ventricle and the origins of the arterial trunks from the right ventricle, were adequately determined with conventional imaging. However, the invaluable additional data was determined with the use of a model. The newly found information formed the basis upon which the surgery to remove the ventriculo infundibular fold in the roof of the interventricular communication, tunnel the defect to the aorta, expand the outflow tract with a patch, and remove band from the pulmonary trunk was planned (Riesenkampff et al. 2009).

Fig 13.showing the 3D model of the right atrium and ventricle of the 20 month old girl mentioned in the above case study

1.8.2. Surgical Models for Training Purposes and Medical Devices

Modelling in medicine has given rise to innovative surgical models for use in training. Surgical training models referred to as Primacorps are produced from imaging data taken by MRI of actual patients. Primacorps training models creates a very realistic

simulation with all the characteristics of an actual patient (Corney and Hieu 2005). The use of modelling has also been applied to the manufacture of medical devices, a method for the production of medical devices designed for controlled release of bioactive agent as well as implantation and cell growth is described with the use of computer aided design (CAD) (Cima and Cima 1996).

1.8.3. Scaffolds for Tissue Engineering

Tissue engineering is based on the production of fully functional tissue for regenerative medicine and drug testing purposes. Modelling with the use of 3D printing in the fabrication of tissue and in some cases the reproduction of an organ has been achieved by printing the structure layer by layer. Scaffold based or scaffold free approaches has also been applied in tissue engineering to provide a biomimetic structural environment to encourage tissue growth and formation which promotes host tissue integration (Richards et al. 2013).

This can be applied where the sample cells are cultured ex vivo using the scaffold for cell and tissue growth, and implanting the cultivated tissue into the patient for functional restoration. The use of imaging such as CT and MRI along with geometrical modelling allows for the scaffolds to be designed for a specific purpose, the use of rapid prototyping then allows the scaffolds to be produced (Peltola et al. 2008; Richards et al. 2013)

Case study

This describes a method that has been used to prepare artificial skin used in treatment of severe burn victims. A housing capable of holding the cells and nutrients for sufficient time to allow for them to form a uniform tissue, this is also applied to bone tissue. The manufacture of these 3D scaffolds made of various materials to house the cell cultures is done by rapid prototyping. Research is being done at The University of Hong Kong to create these scaffolds from biodegradable polymer materials that would allow the scaffold to be replaced by host tissue. It is believed the porous nature of the scaffold would create an environment to facilitate cell anchoring by micro locking, while also encouraging quick cell growth. Hydroxyapatite

can be incorporated into the scaffold to further encourage strong and healthy bone growth. Bone being a complex tissue, which is heterogeneous and directional in terms of its ability to bear load, hence it is difficult to recreate. However, researchers were able to produce samples of bone using rapid prototyping, but none of the samples can be applied in a load bearing capacity (Gibson et al. 2006).

Fig 14. (A) showing the powder for SLS, (B) shows the sintered sample and (C) shows the nylon scaffold.

1.9. Medical Requirements of Rapid Prototyping

Though the usefulness of rapid prototyping in the field of medicine is well recognized, there are still certain limitations which exist because the technology was not specifically created for the area of medicine but rather for the manufacturing sector. Thus there is a need to improve the technology specifically for the area of medicine if it is to reach its true potential and increase its benefit to surgeons. The main areas that are crucial in the medical field and needs to be focused on if RP is to survive as a viable tool to surgeons are:

Speed

These models are known to take anywhere from a couple hours to a couple days to completely produce, the majority of this time is spent processing the imaging and performing segmentations. This processing in most cases takes a greater time than the actual production of the physical model, this limits the application of these models and eliminates them from emergency use.

Cost

Rapid prototyping reduces the cost in manufacturing in bulk, however this same efficiency is not always transferred when used in the medical field. Thus it is not likely

to be utilised in every case, it will be reserved for complex cases where the cost is justified.

Accuracy

Most RP models are highly accurate, in most cases the inaccuracies arise in the imaging modality used to produce the model.

Materials

To truly be useful in the field of medicine the materials used to create these models need to be safe for introduction into the theatre and biocompatible for insertion into the body. This increases cost and limits the applications of models.

Easy to use

Currently the production of models require technical skills and specialized software for segmentation, this increases processing time and cost of production of these models (Gibson et al. 2006).

1.10. Limitations of Rapid Prototyping

An experiment was described to derive the accuracy of different rapid prototyping techniques including laser sintering (SLS), 3D printing (3DP) and PolyJet in the creation of models to be used in the medical field. Models were created of the skull as .SLS, 3D prints and Polyjet models. Measurements were taken using a coordinated measuring machine, which identified the positions of measuring balls placed at locations on the models, and calculating the distances between the mid points of these references and comparing it to the model. For the PolyJet the linear or dimensional error was 0.18 $\pm$ 0.13%, for SLS 0.80 $\pm$ 0.32% and for 3DP 0.69 $\pm$ 0.44% (original model), 0.38 $\pm$ 0.22% (moderate model) and 0.55 $\pm$ 0.37% (worse model). The Polyjet proved to reproduce the anatomy with greater accuracy than either SLS or 3DP (Salmi et al. 2013).

2. Objectives

The main aim of this project is to create 3D model representations of coarctation of the aorta in paediatrics and provide analysis on the clinical relevance of these models for the purpose of assisting in surgical preparation of corrective surgery.

An additional objective is to produce a simple model of blood flow through the coarcted vessel by applying computational fluid dynamics. Allowing for the analysis of wall shear and blood velocities in the aorta.

The main targets this report will achieve are:

- Obtain images CT images of coarctation of the aorta in neonates
- Generate a computational 3D anatomical model based on these images
- Segment the model to the region of interest, which is the narrowing of the vessel
- Create a computational fluid dynamic model
    - Wall shear contour
    - Blood velocity vectors
- Create a 3D physical anatomical model
- Examine the clinical relevance of the physical anatomical model

3. Methodology

3.1. Generating Computational 3D Anatomical Model

Computerised tomography images of coarctation of the aorta were obtained from the Paediatric department of the Southern General Hospital in Glasgow in the form of Dicom files. These image files were anonymized for patient confidentiality, and imported into Mimics 17 (materialise, 2014), using the software, the threshold function was performed on the images and segmentation to isolate the area of interest which was the aorta, specifically at the region of coarctation. This was done with the aid of a surgeon to assist in identifying the specific anatomical structures.

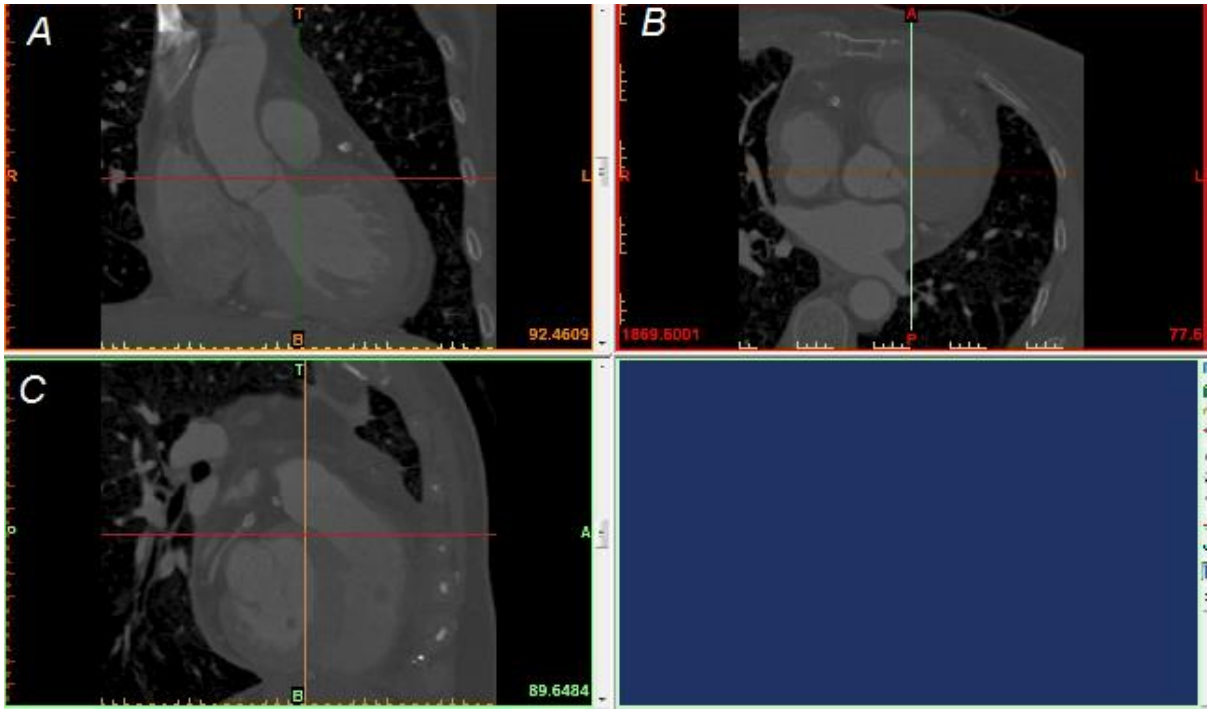

Fig 15. Showing the original unedited Dicom images of the CT scan as it appears in the Mimics software before manipulation. Part A represents the frontal (coronal) plane, Part B the transverse (horizontal) plane and Part C the sagittal plane.

Thresholding generates a mask on the image based on a specified region of shades. The CT images are black and white photos taken using x-ray, these photos depict the anatomy on a grey scale based on the density of the tissue. If the tissue is dense enough, the x-ray beam is reflected and the object appears white in the image, dense tissue such as bone often appear as a lighter shade. However, less dense tissue appear as darker shades because more of the beam is penetrating the object. The

threshold function is able to highlight specific anatomy based on the position on this grey scale, for this project the blood vessels were isolated by thresholding the blood inside, since blood has a similar density to bone.

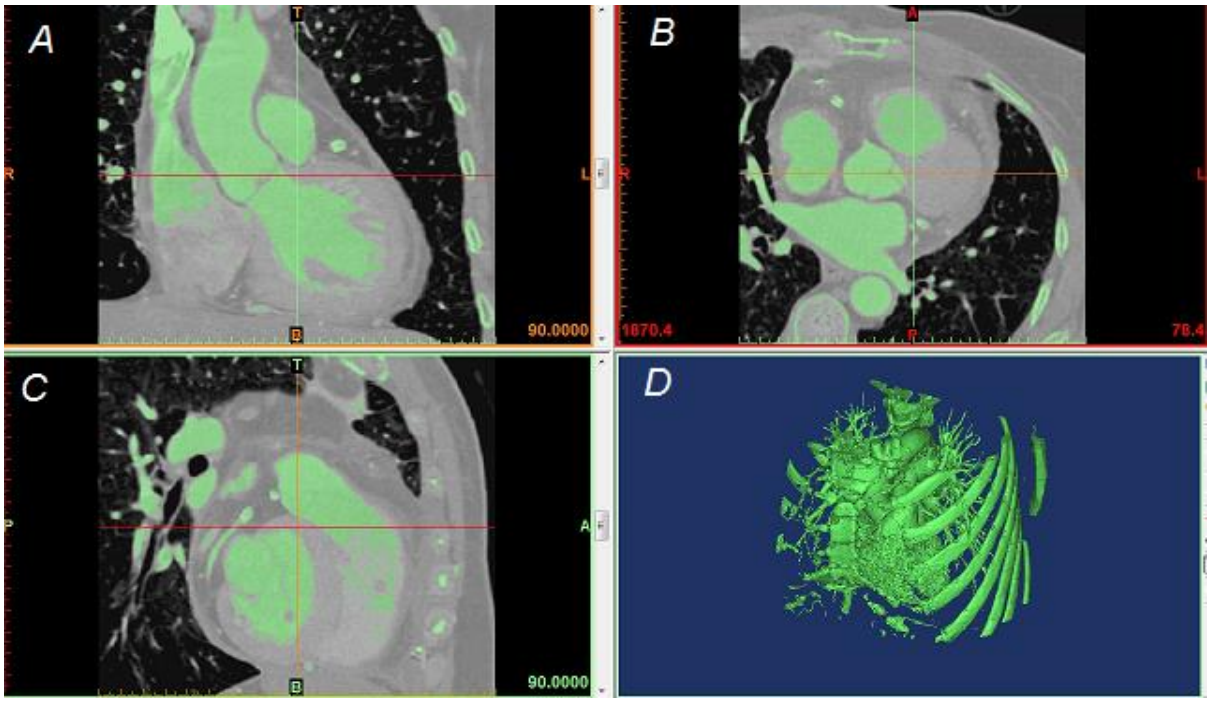

Fig 16. Showing the images after performing thresholding, the green area in each plane is the mask generated based on the grey scale. Part D depicts the 3D representation of the thoracic section of the anatomy generated from the mask in each plane.

Segmentation is the isolation of the area of interest, it involves removing all the anatomy that is irrelevant to the aim while retaining and generating a 3D computational model of the relevant anatomy. The Dicom files contain slices taken by the CT process, the scanner divides the anatomy into very thin layers of the sagittal, coronal and axial planes. Each slice represented by an image, hence the entire scan comprises of numerous images on each plane. To segment the area of interest, each image must be edited individually, the removal of unwanted anatomy from the mask of each slice or image, leaves behind the mask of the region of interest, the final product of this editing is a 3D representation of the anatomy of interest generated from the remaining mask of each image.

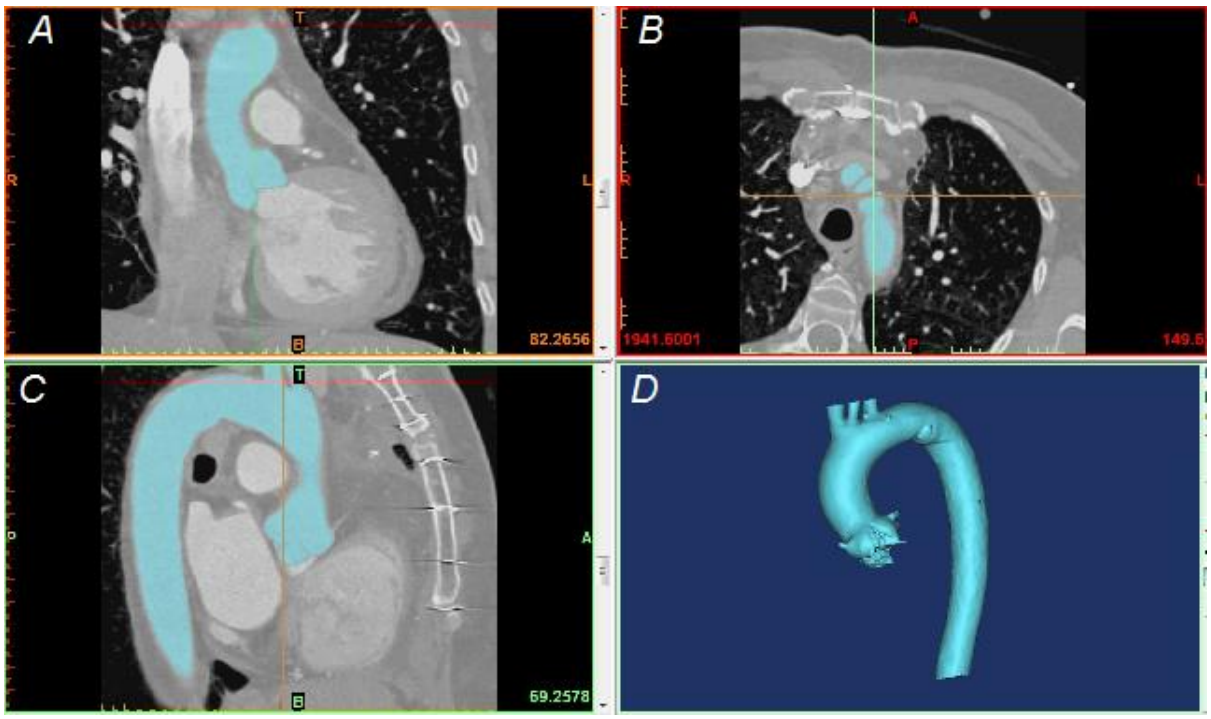

Fig 17. Showing the segmented mask in all three planes, the aorta is singled out as the region of interest. Part D shows the aorta in 3D.

3.2. Computational Fluid Analysis

The geometry in the form of an STL file was imported into ICEM CFD through Ansys workbench 15 (Ansys 2015), a tetrahedral mesh was generated with the global element scale factor autosized to the specific model. The model consisted of an edge criteria of 0.2, with smooth iterations of 5, and a minimum quality of 0.4 producing a total of 125052 elements and 21880 nodes. The inlet and outlet surfaces were created and specified, before exporting the geometry.

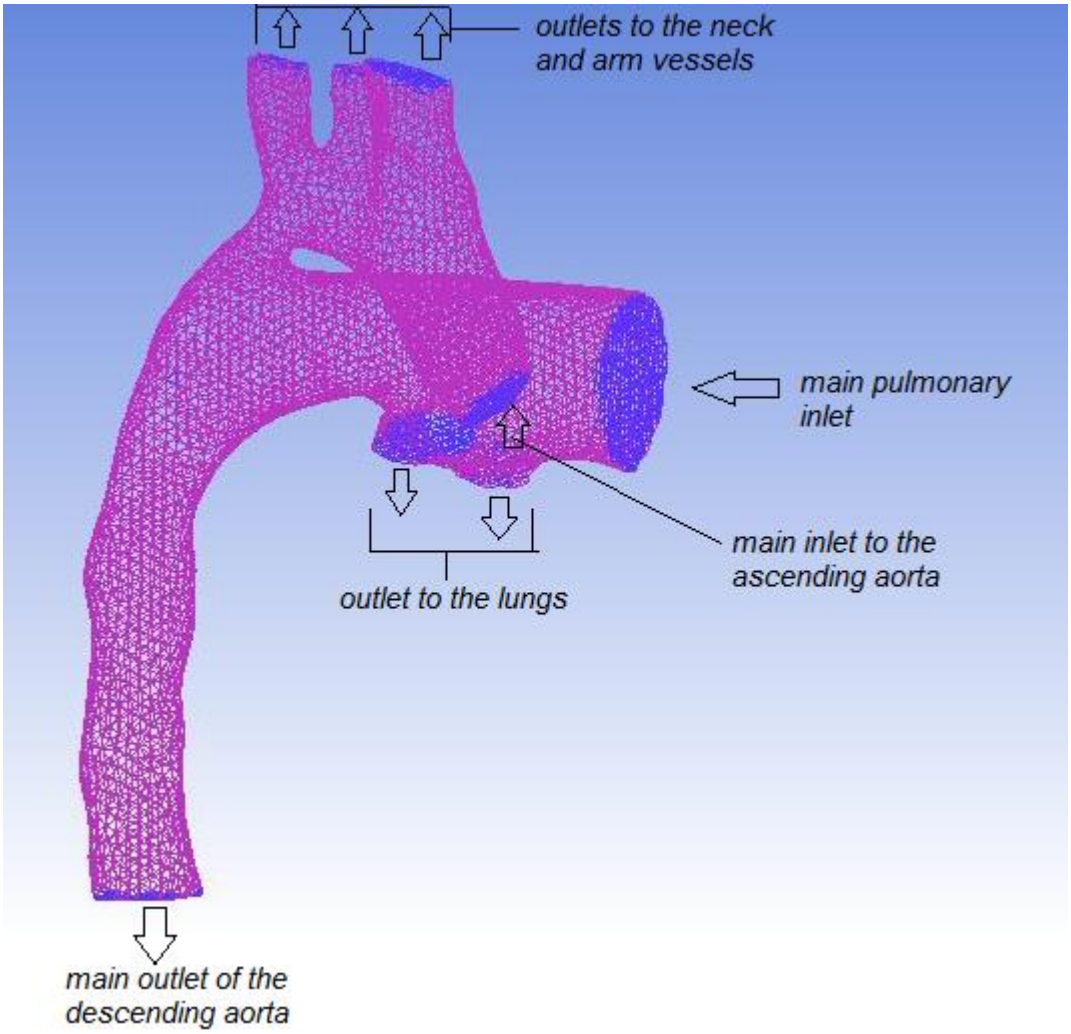

Fig 18. showing the geometry with a tetrahedral mesh, with created surfaces at the inlet and outlets.

The meshed geometry was transferred to Fluent, through workbench as well. In Fluent, the boundary conditions were set based on physiological data found in the literature. For this simple initial analysis the vessel wall was modelled as a rigid body, the density of blood was taken as $1.05 \times 10^3\ kg/m^3$and the blood was modelled as a non-compressible Newtonian fluid with constant viscosity of $4.0 \times 10^{-3}\ Pa.s$ (Pedley and Luo 1995). In the model of the healthy adult aorta, there were numerous values for peak systolic pressure in the aorta directly out of the left ventricle of $\geq 140\ mmHg$ (Pickering et al. 2005; Reichek and Devereux 1982), $92\ Torr\ (92\ mmHg)$ (*Biomechanics of the Cardiovascular System* 1995). The blood in the aorta estimated to reach a peak axial velocity of $1 - 2\ m/s$ (Kilner et al. 1993; Wood et al. 2001). The flow of blood through the carotid, subclavian and

brachiocephalic arterial branches of the aortic arch is estimated to be 5% of the total ejection volume of the left ventricle for each of the vessels (Shahcheraghi et al. 2002). Simple computational fluid dynamic models demonstrating wall shear and blood velocity vectors for the healthy adult human aorta in a state of rest were created using the above data as boundary conditions.

Cardiovascuar homeostasis conditions change in newborns over the first few hours to days after birth, left ventricle output is $327 \pm 66\ mL/min/kg$ up to one hour after birth, it subsequently decreases to $245\ \pm 56\ mL/min/kg$ twenty four hours after birth (Agata et al. 1991). Neonates with coarctation present with an elevated aortic pressure close to 112/70 mmHg and a peak systolic pressure gradient over the narrowing of approximately 20 mmHg, depending on the severity of the narrowed region. Doppler findings show a peak blood flow velocity of $0.7 \pm 0.4\ m/s$ in the aorta of patients with coarctation (Shaddy et al. 1986). In this model the duct connecting the pulmonary circulation to the arterial circulation is still present, thus pulmonary data was also included in the model as boundary conditions. The changes in the pulmonary circulation after birth is quite significant, in newborns approximately 85-90% of the right ventricular ejection volume by passes the lungs and goes through the ductus arteriosus until the duct eventually closes as the newborn matures (Rudolph 1979). In a healthy full term newborn, the pulmonary arterial systolic pressure (PASP) is 20 mmHg at the time of birth, and 39.1 mmHg at four days old, the overall systolic blood pressure is $68.63 \pm 10.9\ mm$ (Gao and Raj 2010; Hu et al. 2015). The above data was applied to the geometry in Ansys as boundary conditions, and a computational fluid dynamic model was generated representing the wall shear and velocity vectors simulated by the flow of blood through the aorta and pulmonary artery.

The model, based on the above data from literature, the main inlet of the ascending aorta was a velocity inlet of 2 m/s, the neck and arm vessels were modelled as outflows with 5% of the total flow entering each vessel. The main pulmonary inlet is a pressure inlet with a gauge pressure of 20 mmHg, the main outlet of the descending aorta is a pressure outlet with a gauge pressure of 84 mmHg. The pulmonary

branches to the lungs were also modelled as outflows, with 10% of the flow in the main pulmonary artery going to each lung. All values chosen are consistent with the range specified in literature.

3.3. Printing Anatomical Structures

The 3D image was transferred to 3-Matic 8 software (Materialise, Leuven, Belgium), here the images were cleaned up by smoothing and wrapping to ensure that they were ready for printing by making them complete solid structures with no holes. The objects were hollowed to the dimensional thickness of a human aorta at the neonate stage, and exported as a stereolithography (STL) file ready for printing.

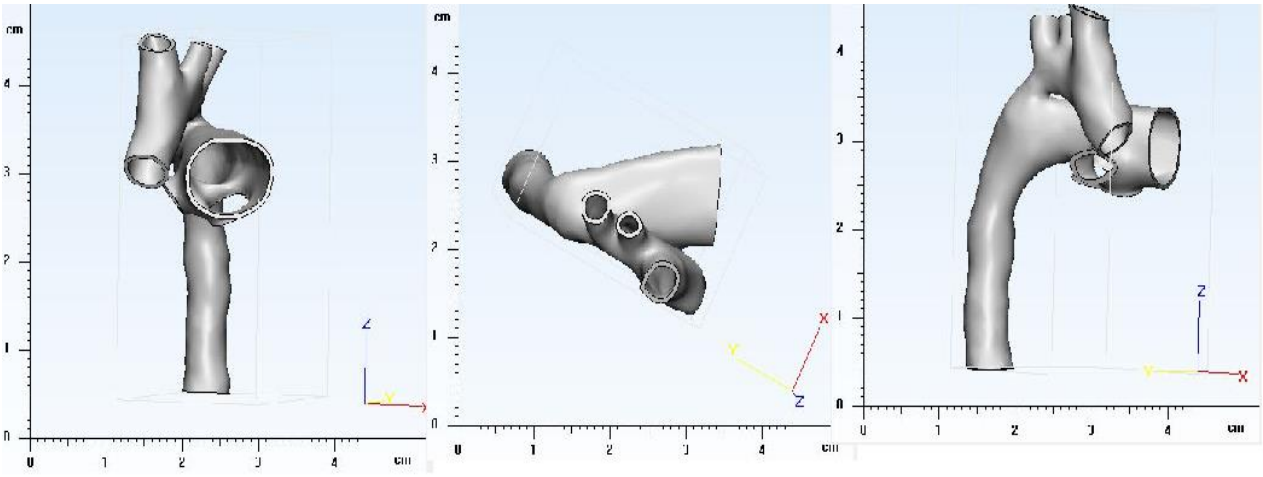

Fig. 19 showing the final image in 3-Matic that is exported for printing as an STL file. The image have been smoothed to reduce roughness on the surface, they have also been hallowed and the ends trimmed for a clean finish.

The STL files were imported into Magics (Materialise 2015), here the images were prepped for printing by creating a support structure to prevent the model from collapsing during the printing process. The created supports provide a foundation on which to build the model, because the models are produced by a compilation of layers, any overhanging layers must have a structural support to prevent it collapsing and causing a failure during printing. An estimated gap or overhang of 3mm can be supported on its own without the use of reinforcement.

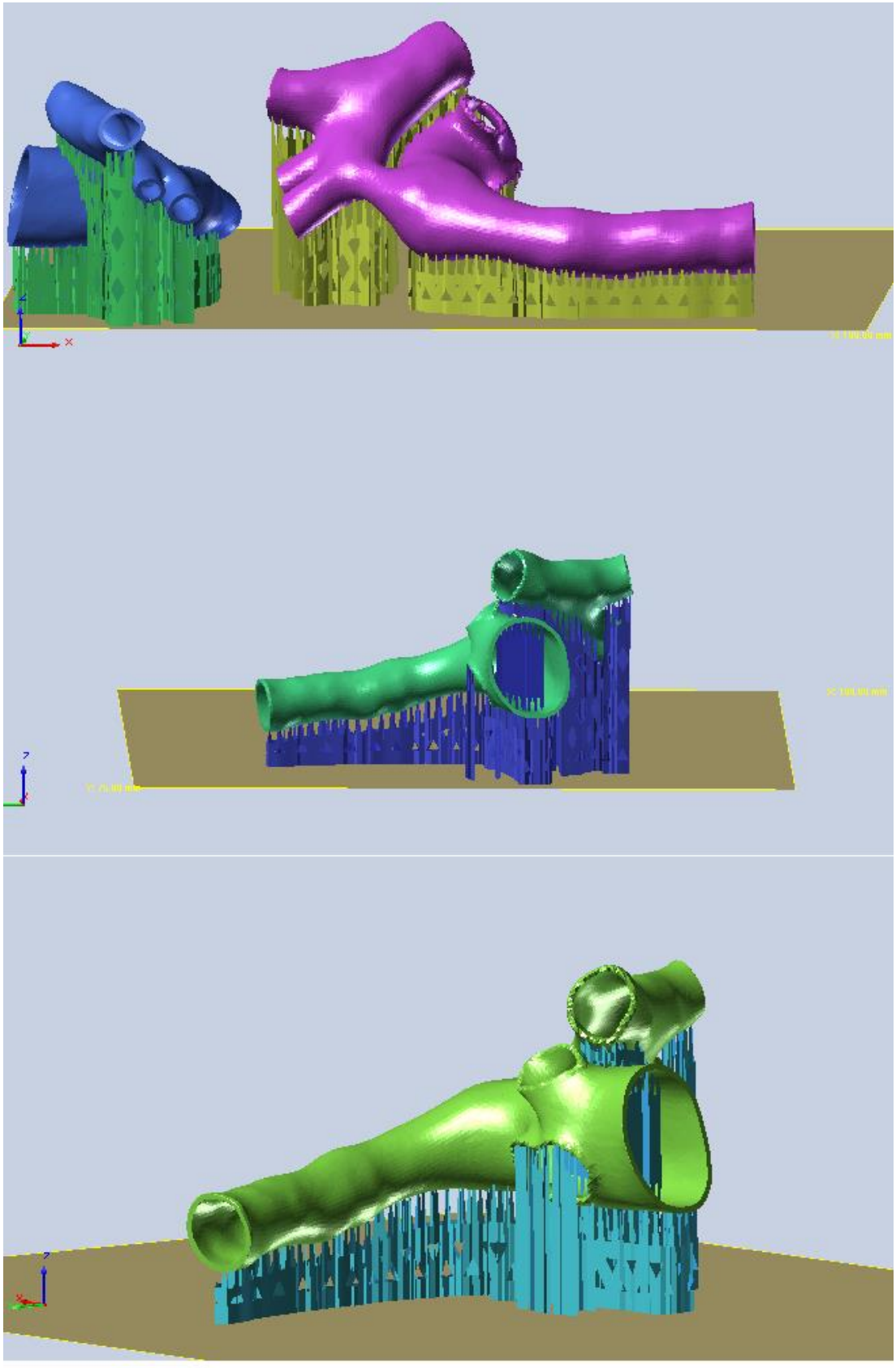

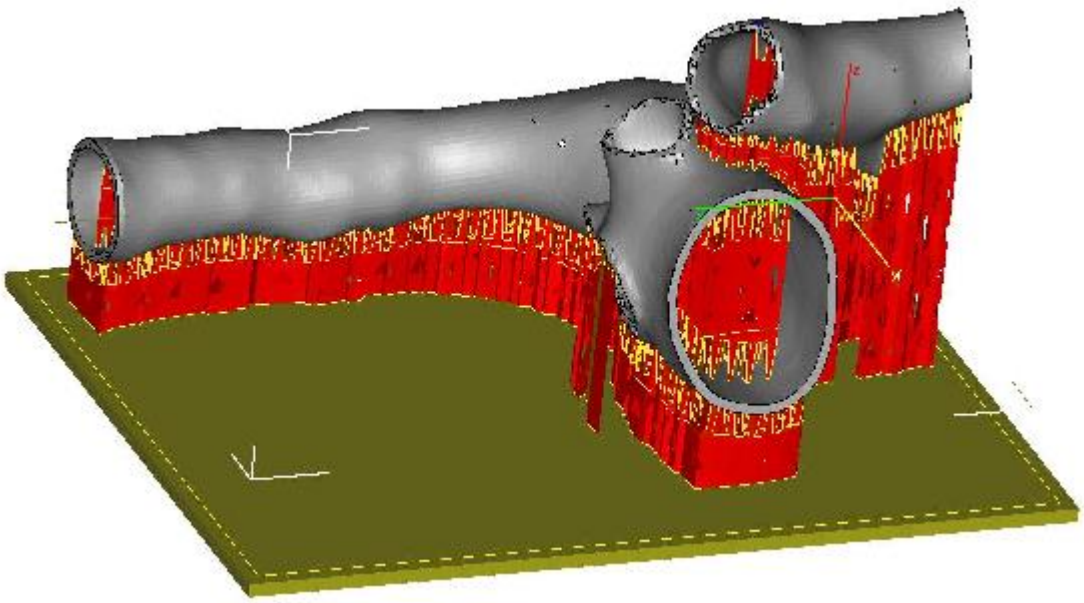

Fig. 20 showing the added structural supports, the platform and the model. Notice the supports are not only on the exterior but are strategically placed on the interior for additional reinforcement.

The models were printed using two different printers, the Perfactory® Desktop Digital Shell Printer (Envisiontec) (see Appendix 1, fig. 29), and the Object Eden 350. The DDSP printer created the model using HTM140-V2 (high temperature material) (see Appendix 1, fig. 30), while the models from the other printer were printed in ABS (Acrylonitrile-Butadiene-Styrene) material. HTM140 and its variations are a set of variable resins associated with Envisiontec products and known for toughness, these material is versatile and can be made to fit most applications. The material is a Simulated Engineering Plastic, which means that its most pronounced properties are durability and the ability to tolerate very high temperatures. It is a material that can be moulded from a cast or even used as a master. Models created with this material are able to survive the vulcanization process in rubber at high temperatures and pressures while maintaining its structural integrity, dimensions and intricate detail. The material has a tensile strength of 56 MPa and a flexural strength of 115 MPa, this material can also be used in a variety of applications. It is able to be painted, adding to its applications in manufacture or as a visual aid. It is considered one of the most versatile and high performing materials in 3D printing today, mainly because the level of quality of the surface finish allowing it to produce intricate details (Envisiontec

2015). ABS is an affordable engineering thermoplastic known for its resilience to degradation from chemicals, heat or impact. It is generally applied in machined prototypes, structural components, housings and support blocks because of the ease in which it is machined and fabricated. Its characteristics include good machinability, excellent aesthetics, strength and stiffness, easy to paint and glue and dimensional. Available in a natural beige or black, it is compliant for use in in the rapid prototyping industry, at room temperature (23 c^{o}) the flexural modulus is 330,000 psi, and the flexural strength at yield is 9,500 psi with a compressive strength of 7,650 psi. (Ecreativeworks 2015).

After the models were printed, they were removed from the machine and blasted with compress air to remove excess resin from the object. They were then washed in a bath of isopropanol and allowed to dry. After drying the resin was cured with the use of ultraviolet light to harden the models, the support structures were then removed with the use of a blade and a small screwdriver leaving the complete model behind.

Fig 21. showing the models upon completion just as they are raised from the pool of resin.

Fig 22. showing the models as they are being removed from the platform on which they were made. At this point the three models are connected by a thin layer of solidified resin on the platform.

Fig 23. showing the completed models still connected and glistening in the light due to excess resin still on them.

Fig 24. showing the models being washed in a bath of isopropanol and left do dry on a paper towel.

Fig. 25 showing the removal of the supports added prior to printing in order to provide the necessary reinforcement during synthesis. The removal of these supports leave the completed model behind.

4. Results

4.1. Computational Fluid Dynamics (CFD)

Table 1 below shows the values obtained for maximum velocity and pressure at each inlet and outlet.

	Maximum velocity (m/s)	Maximum pressure (mmHg)
Pulmonary inlet	2.34	20*
Main outlet from descending aorta	4.04	84*
Main inlet to ascending aorta	2.0*	110.62
Subclavian outlet	0.33	11.10
Carotid artery outlet	0.46	109.01
Brachiocephalic outlet	0.60	109.03
Pulmonary outlet to lung 1	1.97	26.42
Pulmonary outlet to lung 2	2.05	22.22

Table 1. Key: * indicates values entered as boundary conditions.

The maximum wall shear stress recorded throughout the model is $2.7 \times 10^{-3}\ mmHg$, the maximum blood velocity recorded at any point is $6.97\ m/s$.

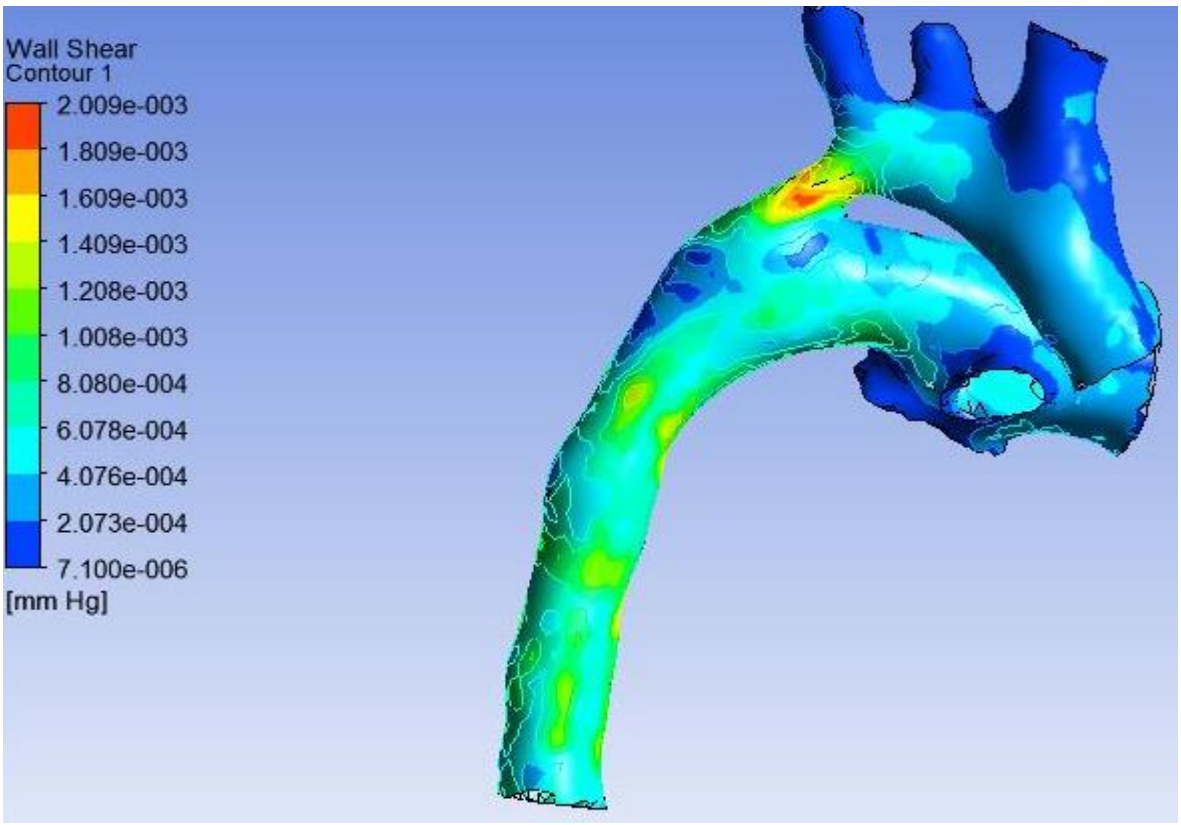

Fig. 26 showing the contour of wall shear stress with the associated legend on the coarcted aorta of the neonate. Area in red indicate high wall shear stress, this can be seen at the area of coarctation.

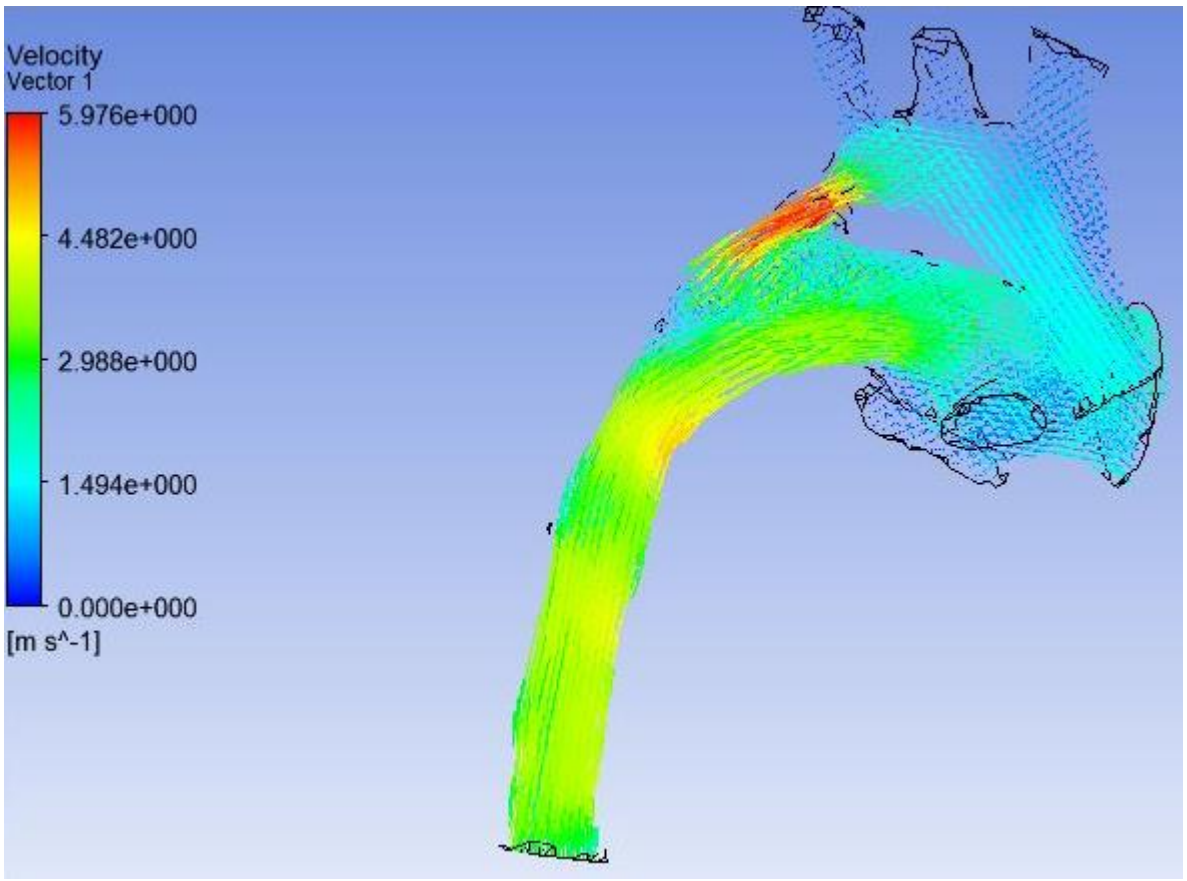

Fig 27. showing the velocity vectors with the associated legend of the blood flowing through the aorta. Areas in red show elevated blood velocity level particularly in the area of the coarctation.

4.2. Printed Anatomical Model

Fig. 28 showing the finished printed model of coarctation of the aorta.

5. Discussion

The models, both the printed and CFD, originated from a CT scan performed on a 10 day old neonate. The patient presented clinically with cardiovascular compromise, reduced femoral pulses and acidosis. The patient was stabilised with prostaglandin infusion to prevent ischemia by adequately maintaining blood flow to the lower body through the ductus arteriosus.

The diagnosis was confirmed with the use of echocardiography, aortic coarctation with aortic arch hypoplasia. A CT scan was performed to provide additional information detailing the arch anatomy. The patient subsequently underwent a successful surgical repair for the coarctation of the aorta.

5.1. Computational fluid dynamics

The CFD models were created using simplified mathematical models of both the blood and the anatomical model. The blood was modelled as a Newtonian fluid with constant density and viscosity, in reality both these parameters may vary from patient to patient. Also blood is not a Newtonian fluid, the viscosity not only varies depending on the patient, it is also not a constant the viscosity of blood is shear rate dependent. However, despite these limitations these simple models have served their purpose and highlighted some key issues with coarctation of the aorta. One such issue is the point of maximum recorded wall shear of $2.7 \times 10^{-3}\ mmHg$, which was at the location of the coartation, more specifically at the most narrowed region. This elevated shear stress can cause damage to the vessel wall, and the components of the blood through adverse haemodynamics. Another issue is elevated blood velocity levels also in the area of the narrowing, this is expected because a force is pushing a volume through a narrowed region, the result will be an increase in velocity. These conditions can cause haemolysis (rupture of the red blood cells) leading to haemolytic anaemia, a depletion of red blood cells in blood. The data obtained from CFD shows elevated blood pressure levels in the upper body, the average blood pressure levels through the neck vessel branches of the aortic arch is 110 mmHg, however the blood pressure at the level of the outlet of the descending aorta is 84 mmHg. This gives a

residual gradient across the region of coarctation which is consistent with the literature, this also suggest that the lower body is not very well perfused which may lead to ischemia. The findings of the data from CFD are consistent with literature, except for the blood velocities, we have recorded higher than expected blood velocities, and this may be a result of the simplicity of the model with the use of a Newtonian representation for blood. The CFD provides additional data that may be of assistance to surgeons on planning the surgery or assessing the success of the surgery through obtaining residual gradients and wall stress. In the future a more realistic model may be created with the use of velocity profiles at the inlet to simulate systole and diastole, also modelling blood as a non-Newtonian fluid with a variable viscosity. The wall may also be modelled as a deformable body instead of a rigid body for completeness, these modifications would provide a more realistic representation of the flow of blood in a coarcted aorta.

5.2. Physical Model

One of the benefits of this type of modelling is that the anatomy can be reproduced quickly, and accurately. This gives surgeons real time access to the necessary planning tools in order to prepare for the surgery. It is estimated, a completed printed model can be produced in a day, the printing process takes approximately three hours, providing the segmentation and other preparatory work can be done in a timely manner, the process can be completed in a matter of hours. This is extremely advantageous in the area of surgical planning, it provides the surgeon with an additional tool which can be created in a reasonable time frame.

The models created were analysed and appraised by Mark HD Danton, a Consultant Paediatric Cardiac Surgeon. The model was printed with great detail, the ductus arteriosus, the ascending aorta, the main pulmonary artery and its braches to the lungs, the region of coarctation and the descending aorta could all be clearly identified even to the untrained eye, a clear advantage over the current imaging modalities This is a view also shared with Mr Danton, “The model is in true scale, and describes the arch and ductal anatomy. Clearly seen is the ascending aorta [6mm]

Arch - proximal [6mm], - distal [5mm]. The CoA is pre-ductal in site i.e. isthmus region. The proximal main pulmonary artery is evident [10mm] and the bifurcation into left and right pulmonary arteries is evident. Interestingly LPA = 8 mm max diameter, whereas RPA = 5 mm. This difference in pulmonary artery calibre has not been recognised on previous investigation. From the bifurcation leads the patent Ductus Arteriosus connecting pulmonary artery to descending aorta, 7mm in diameter". The model was printed 1:1, meaning it was printed to the actual size of the art in the neonate of 10 days old, which is quite small, in fig. 25, this can be clearly seen in comparison with the fingers. An upscale version of the anatomy was also printed, this showed the anatomy much more clearly, it is useful as a teaching tool however as for as clinical relevance the clinician thought it better to have the models to the actual size of the patient.

In his appraisal Mr Danton highlighted some relevant clinical areas where the models may be utilised to assist surgeons in planning their operation. One of the advantages of the model he highlighted was "the model demonstrated very close correlation in morphology to the true anatomy as seen at surgical repair. The quality is outstanding, all key anatomical structures are clearly recognisable". Clinical areas outlined for which this model would be extremely useful are application in resolving the surgical approach, whether a sternotomy with cardiopulmonary bypass (CPB) or a thoracotomy would be the better approach to accessing the coarcted site. He suggested the model would also be useful in the determining the repair method, whether a simple excision of CoA would suffice or further extended resection is needed. Also if subclavian flap repair is the ideal method or balloon angioplasty with stenting, this model could give further insight to make these critical judgment calls. From the model provided, the experienced consultant surgeon decided on a subclavian flap repair through a thoractomy would be ideal "From the model, I would anticipate a repair via thoractomy would be possible; however augmentation of distal arch with subclavian flap is likely." He went on to state that "Typically this lesion would be treated surgically however if the baby was unfit for an operation an alternative might be to place a stent in the Ductus arteriosus, in order to temporise

and allow a delayed repair when the baby was fit. This would be a rarely considered option, only under exceptional circumstances." This model will prove most beneficial in the planning and determination of stent size for balloon angioplasty. Currently stent diameter and length are determined during surgery, after the patient is put under the knife and the surgeon can inspect and analyse the vessel, there is clearly a need for greater planning in this area because the dimensions of the stent need to be accurate, too long or to short may have adverse effects. This model provides the surgeon with a way to determine stent diameter, length and pressure at which to expand the balloon during implantation before the operation reducing the risk of a miss fit. This was a point outlined by Mr Danton "The model provides an excellent template for planning stent implantation." From the model he was able to determine anatomical measurements needed to perform balloon angioplasty and make inferences on the length of the stent needed, "The length of the duct can be accurately measured – inferior curve – 10mm, superior curve =7mm. The proximal landing zone can be carefully evaluated, in particular the origin of the LPA, which is distal to the origin of RPA, by 1-2 mm. The distal landing zone is complex because the inferior component is longer than the superior aspect. Simple, standard stent designs do not accommodate these individualised complexities and a compromise stent length needs to be made. If the stent is too long this may compromise flow in the isthmus region, too short ductal tissue will not be covered with a risk of stenosis on prostin cessation." The model enabled him to determine vessel diameters to conclusively decide upon the diameter of the stent "the duct external diameter = 7mm, therefore a stent diameter should be = 7mm or less." Models like this may lead to stents being customized for each patient, ensuring an exact fit "Ultimately this model would allow a bespoke stent manufacture to fit exactly the individualised anatomical constraints of this particular patient."

The future of anatomical modelling may provide surgeons with a far greater planning tool than currently provided from imaging modalities, this may reduce surgical mistakes in the operating theatre and increase survival rates of high risk procedures through advance planning and teaching that can be provided by these models. Mr

Danton in his appraisal gave his opinion on the future benefits of such a technology "one may be able to use this model as a test bed for stent implantation. Using a clear [and perhaps compliant material] various stent designs and lengths might be 'tested' and the optimal solution defined prior to the intervention on the baby. This would reduce guess-work, trial-and-error judgements thereby reducing procedural time, exposure to radiation, stent wastage."

The only expected expense in producing the computational model will be obtaining the necessary software licenses, while for the 3D model, initial capital cost of obtaining the software licenses, the printer and material will be expensive. However after this initial cost, maintenance of the machine and material will be the only expenditure

5.3. Limitations

This report only analysis one model, originally three models were segmented and prepared for printing, however due to ethical reasons only one model could be printed for this report. The three models were all of coarctation, the model included here of severe coarctation with the pulmonary artery connected to the aorta by the duct, a less severe case with a disconnected duct and a model after the repair procedure by the subclavian flap method. The actual images of segmentation for the model created and discussed in this report could not be obtained. As a result of these limitations, the images in Fig 15-17 are of a healthy adult, as these images did not require ethical approval.

6. Conclusion

The models created have proven to provide additional information that could not be previously obtained with the use of conventional imaging modalities. Computational fluid analysis has provided contour of wall shear stress and blood velocity vectors, which can be useful in fully understanding the legion produced by coarctation of the aorta and how in impacts the haemodynamics of the blood. The physical anatomical models provide much needed detail of the anatomy, this is extremely beneficial in the planning process for surgeons, and the models are produced in a reasonable time giving this the realistic potential to be part of the planning for complex surgery. One drawback to the implementation of this technique, is the cost, particularly the initial cost, this may cause hospitals to reserve this technique for isolated complex cases rather than implement it mainstream. Regardless of how it is implemented this technique has proven to be very useful in the eyes an experienced consultant cardiac surgeon.

References

1. Agata, Youtaro, Satoshi Hiraishi, Koki Oguchi, Hitoshi Misawa, Yasunori Horiguchi, Nobuyuki Fujino, Kimio Yashiro, and Nobuhiro Shimada. 1991. “Changes in Left Ventricular Output from Fetal to Early Neonatal Life.” *The Journal of Pediatrics* 119 (3): 441–45. doi:10.1016/S0022-3476(05)82060-8.

2. Allen, Bradley D, Alex J Barker, James C Carr, Robert A Silverberg, and Michael Markl. 2013. “Time-Resolved Three-Dimensional Phase Contrast MRI Evaluation of Bicuspid Aortic Valve and Coarctation of the Aorta.” *European Heart Journal Cardiovascular Imaging* 14 (4): 399. doi:10.1093/ehjci/jes225.

3. Backer, C. L., K. Paape, V. R. Zales, T. J. Weigel, and C. Mavroudis. 1995. “Coarctation of the Aorta : Repair With Polytetrafluoroethylene Patch Aortoplasty.” *Circulation* 92 (9): 132–36. doi:10.1161/01.CIR.92.9.132.

4. Backer, Carl L, Constantine Mavroudis, Elias A Zias, Zahid Amin, and Thomas J Weigel. 1998. “Repair of Coarctation with Resection and Extended End-to-End Anastomosis.” *The Annals of Thoracic Surgery* 66 (4). Elsevier: 1365–70. doi:10.1016/S0003-4975(98)00671-7.

5. Baker, E J, V Ayton, M A Smith, J M Parsons, M N Maisey, E J Ladusans, R H Anderson, M Tynan, A K Yates, and P B Deverall. 1989. “Magnetic Resonance Imaging of Coarctation of the Aorta in Infants: Use of a High Field Strength.” *Heart* 62 (2): 97–101. doi:10.1136/hrt.62.2.97.

6. Barreiro, Christopher J, Trevor A Ellison, Jason A Williams, Megan L Durr, Duke E Cameron, and Luca A Vricella. 2007. “Subclavian Flap Aortoplasty: Still a Safe, Reproducible, and Effective Treatment for Infant Coarctation.” *European Journal of Cardio-Thoracic Surgery : Official Journal of the European Association for Cardio-Thoracic Surgery* 31 (4): 649–53. doi:10.1016/j.ejcts.2006.12.038.

7. Ben Saad, Moez, Adela Rohnean, Anne Sigal-Cinqualbre, Ghazal Adler, and Jean-Francois Paul. 2009. “Evaluation of Image Quality and Radiation Dose of Thoracic and Coronary Dual-Source CT in 110 Infants with Congenital Heart Disease.” *Pediatric Radiology* 39 (7): 668–76. doi:10.1007/s00247-009-1209-6.

8. Bentham, J R, and J D R Thomson. 2015. “Current State of Interventional Cardiology in Congenital Heart Disease.” *Archives of Disease in Childhood*, February, archdischild – 2014–306052 – . doi:10.1136/archdischild-2014-306052.

9. *Biomechanics of the Cardiovascular System*. 1995. Czech Technical University Press. https://books.google.co.uk/books/about/Biomechanics_of_the_Cardiovascular_Syste.html?id=_fY5AAAACAAJ&pgis=1.

10. Chua, Chee Kai, Kah Fai Leong, and Chu Sing Lim. 2010. *Rapid Prototyping: Principles and Applications*. World Scientific. https://books.google.co.uk/books/about/Rapid_Prototyping.html?id=4OYcyiDUpsQC&pgis=1.

11. Cima, LG, and MJ Cima. 1996. “Computer Aided Design; Stereolithography, Selective Laser Sintering, Three-Dimensional Printing.” *US Patent 5,490,962*. https://www.google.com/patents/US5490962.

12. Corney, J, and LC Hieu. 2005. “Medical Rapid Prototyping Applications and Methods.” *Assembly …*. http://www.emeraldinsight.com/doi/pdf/10.1108/01445150510626415.

13. Cramer, Jonathan W, Salil Ginde, Peter J Bartz, James S Tweddell, S Bert Litwin, and Michael G Earing. 2013. “Aortic Aneurysms Remain a Significant Source of Morbidity and Mortality after Use of Dacron(®) Patch Aortoplasty to Repair Coarctation of the Aorta: Results from a Single Center.” *Pediatric Cardiology* 34 (2): 296–301. doi:10.1007/s00246-012-0442-1.

14. Didier, D, C Saint-Martin, C Lapierre, P T Trindade, N Lahlaidi, J P Vallee, A Kalangos, B Friedli, and M Beghetti. “Coarctation of the Aorta: Pre and Postoperative Evaluation with MRI and MR Angiography; Correlation with Echocardiography and Surgery.” *The International Journal of Cardiovascular Imaging* 22 (3-4): 457–75. doi:10.1007/s10554-005-9037-8.

15. Ecreativeworks. 2015. *Plastics International.* Accessed July 2015. http://www.plasticsintl.com/abs.htm.

16. Envisiontec. 2015. *Envisiontec.* Accessed July 2015. http://envisiontec.com/material-htm-140/.

17. Fletcher, B D, and M D Jacobstein. 1986. “MRI of Congenital Abnormalities of the Great Arteries.” *AJR. American Journal of Roentgenology* 146 (5). American Roentgen Ray Society: 941–48. doi:10.2214/ajr.146.5.941.

18. Friedman, A H, and J T Fahey. 1993. “The Transition from Fetal to Neonatal Circulation: Normal Responses and Implications for Infants with Heart Disease.” *Seminars in Perinatology* 17 (2): 106–21. http://europepmc.org/abstract/med/8327901.

19. Galvan, Cynthia, Emile A. Bacha, Julie Mohr, and Paul Barach. 2005. “A Human Factors Approach to Understanding Patient Safety during Pediatric Cardiac Surgery.” *Progress in Pediatric Cardiology* 20 (1): 13–20. doi:10.1016/j.ppedcard.2004.12.001.

20. Gao, Yuansheng, and J Usha Raj. 2010. “Regulation of the Pulmonary Circulation in the Fetus and Newborn.” *Physiological Reviews* 90 (4): 1291–1335. doi:10.1152/physrev.00032.2009.

21. Gawande, Atul A, Michael J Zinner, David M Studdert, and Troyen A Brennan. 2003. “Analysis of Errors Reported by Surgeons at Three Teaching Hospitals.” *Surgery* 133 (6): 614–21. doi:10.1067/msy.2003.169.

22. Gibson, I., L.K. Cheung, S.P. Chow, W.L. Cheung, S.L. Beh, M. Savalani, and S.H. Lee. 2006. “The Use of Rapid Prototyping to Assist Medical Applications.” *Rapid Prototyping Journal* 12 (1). Emerald Group Publishing Limited: 53–58. doi:10.1108/13552540610637273.

23. Goo, Hyun Woo, In-Sook Park, Jae Kon Ko, Yong Hwue Kim, Dong-Man Seo, Tae-Jin Yun, Jeong-Jun Park, and Chong Hyun Yoon. 2003. “CT of Congenital Heart Disease: Normal Anatomy and Typical Pathologic Conditions.” *Radiographics : A Review Publication of the Radiological Society of North America, Inc* 23 Spec No (October). Radiological Society of North America: S147–65. doi:10.1148/rg.23si035501.

24. Goo, Hyun Woo, In-Sook Park, Jae Kon Ko, Young Hwee Kim, Dong-Man Seo, and Jeong-Jun Park. “Computed Tomography for the Diagnosis of Congenital Heart Disease in Pediatric and Adult Patients.” *The International Journal of Cardiovascular Imaging* 21 (2-3): 347–65; discussion 367. doi:10.1007/s10554-004-4015-0.

25. Haramati, Linda B, Julie S Glickstein, Henry J Issenberg, Nogah Haramati, and Gregory A Crooke. 2002. “MR Imaging and CT of Vascular Anomalies and Connections in Patients with Congenital Heart Disease: Significance in Surgical Planning.” *Radiographics : A Review Publication of the Radiological Society of North America, Inc* 22 (2). Radiological Society of North America: 337–47; discussion 348–49. doi:10.1148/radiographics.22.2.g02mr09337.

26. Harrison, D A. 2001. “Endovascular Stents in the Management of Coarctation of the Aorta in the Adolescent and Adult: One Year Follow up.” *Heart* 85 (5): 561–66. doi:10.1136/heart.85.5.561.

27. Hoffman, Julien I.E, and Samuel Kaplan. 2002. “The Incidence of Congenital Heart Disease.” *Journal of the American College of Cardiology* 39 (12). Journal of the American College of Cardiology: 1890–1900. doi:10.1016/S0735-1097(02)01886-7.

28. Hu, Qian, Wei D Ren, Jian Mao, Juan Li, Wei Qiao, Wen J Bi, Yang J Xiao, et al. 2015. “Changes in Pulmonary Artery Pressure during Early Transitional Circulation in Healthy Full-Term Newborns.” *Ultrasonics* 56 (February): 524–29. doi:10.1016/j.ultras.2014.10.005.

29. Ing, Frank F., Thomas J. Starc, Sylvia P. Griffiths, and Welton M. Gersony. 1996. “Early Diagnosis of Coarctation of the Aorta in Children: A Continuing Dilemma.” *Pediatrics* 98 (3): 378–82. http://pediatrics.aappublications.org/content/98/3/378.short.

30. Jenkins, Kathy J., Kimberlee Gauvreau, Jane W. Newburger, Thomas L. Spray, James H. Moller, and Lisa I. Iezzoni. 2002. “Consensus-Based Method for Risk Adjustment for Surgery for Congenital Heart Disease.” *The Journal of Thoracic and Cardiovascular Surgery* 123 (1): 110–18. doi:10.1067/mtc.2002.119064.

31. Kai, Chua Chee, Chou Siaw Meng, Lin Sing Ching, Eu Kee Hoe, and Lew Kok Fah. 1998. “Rapid Prototyping Assisted Surgery Planning.” *The International Journal of Advanced Manufacturing Technology* 14 (9): 624–30. doi:10.1007/BF01192281.

32. Kaushal, Sunjay, Carl L Backer, Jay N Patel, Shivani K Patel, Brandon L Walker, Thomas J Weigel, Guy Randolph, David Wax, and Constantine Mavroudis. 2009. “Coarctation of the Aorta: Midterm Outcomes of Resection with Extended End-to-End Anastomosis.” *The Annals of Thoracic Surgery* 88 (6): 1932–38. doi:10.1016/j.athoracsur.2009.08.035.

33. Kilner, P. J., G. Z. Yang, R. H. Mohiaddin, D. N. Firmin, and D. B. Longmore. 1993. “Helical and Retrograde Secondary Flow Patterns in the Aortic Arch Studied by Three-Directional Magnetic Resonance Velocity Mapping.” *Circulation* 88 (5): 2235–47. doi:10.1161/01.CIR.88.5.2235.

34. Ladisa, John F, Charles A Taylor, and Jeffrey A Feinstein. 2010. “AORTIC COARCTATION: RECENT DEVELOPMENTS IN EXPERIMENTAL AND COMPUTATIONAL METHODS TO ASSESS TREATMENTS FOR THIS SIMPLE CONDITION.” *Progress in Pediatric Cardiology* 30 (1): 45–49. doi:10.1016/j.ppedcard.2010.09.006.

35. Lee, Edward Y., Marilyn J. Siegel, Charles F. Hildebolt, Fernando R. Gutierrez, Sanjeev Bhalla, and Juliet H. Fallah. 2012. “MDCT Evaluation of Thoracic Aortic Anomalies in Pediatric Patients and Young Adults: Comparison of Axial, Multiplanar, and 3D Images.” *American Journal of Roentgenology*. American Roentgen Ray Society. http://www.ajronline.org/doi/abs/10.2214/ajr.182.3.1820777.

36. Lee, M, Y d’Udekem, and C Brizard. 2014. “Coarctation of the Aorta.” *Pediatric and Congenital Cardiology, …*. http://link.springer.com/10.1007%2F978-1-4471-4619-3_27.

37. Liang, Xin, Ivo Lambrichts, Yi Sun, Kathleen Denis, Bassam Hassan, Limin Li, Ruben Pauwels, and Reinhilde Jacobs. 2010. “A Comparative Evaluation of Cone Beam Computed Tomography (CBCT) and Multi-Slice CT (MSCT). Part II: On 3D Model Accuracy.” *European Journal of Radiology* 75 (2): 270–74. doi:10.1016/j.ejrad.2009.04.016.

38. Meier, M A, F A Lucchese, W Jazbik, I A Nesralla, and J T Mendonça. 1986. “A New Technique for Repair of Aortic Coarctation. Subclavian Flap Aortoplasty with Preservation of Arterial Blood Flow to the Left Arm.” *The Journal of Thoracic and Cardiovascular Surgery* 92 (6): 1005–12. http://europepmc.org/abstract/med/3784584.

39. Melbourne, The Royal Children’s Hospital. 2015. “Cardiology : Coarctation of the Aorta HD.” Accessed August 2. http://www.rch.org.au/cardiology/heart_defects/Coarctation_of_the_Aorta_HD/.

40. Meyer, Richard A., and Samuel Kaplan. 1973. “Noninvasive Techniques in Pediatric Cardiovascular Disease.” *Progress in Cardiovascular Diseases* 15 (4). Elsevier: 341–67. doi:10.1016/S0033-0620(73)80016-7.

41. Moor, Gordon F., Marian I. Ionescu, and Donald N. Ross. 1972. “Surgical Repair of Coarctation of the Aorta by Patch Grafting.” *The Annals of Thoracic Surgery* 14 (6). Elsevier: 626–30. doi:10.1016/S0003-4975(10)65275-7.

42. Murphy, P. J. 2005. “The Fetal Circulation.” *Continuing Education in Anaesthesia, Critical Care & Pain* 5 (4): 107–12. doi:10.1093/bjaceaccp/mki030.

43. Nie, P, X Wang, Z Cheng, Y Duan, X Ji, J Chen, and H Zhang. 2012. “The Value of Low-Dose Prospective ECG-Gated Dual-Source CT Angiography in the Diagnosis of Coarctation of the Aorta in Infants and Children.” *Clinical Radiology* 67 (8): 738–45. doi:10.1016/j.crad.2011.12.007.

44. Noorani, Rafiq. 2006. *Rapid Prototyping: Principles and Applications*. Wiley. https://books.google.com/books?id=eBIfAQAAIAAJ&pgis=1.

45. Pedley, TJ, and XY Luo. 1995. “Fluid Mechanics of Large Blood Vessels.” http://eprints.gla.ac.uk/49910/.

46. Peltola, Sanna M., Ferry P. W. Melchels, Dirk W. Grijpma, and Minna Kellomäki. 2008. “A Review of Rapid Prototyping Techniques for Tissue Engineering Purposes.” *Annals of Medicine* 40 (4). Informa UK Ltd UK: 268–80. doi:10.1080/07853890701881788.

47. Pickering, Thomas G, John E Hall, Lawrence J Appel, Bonita E Falkner, John Graves, Martha N Hill, Daniel W Jones, Theodore Kurtz, Sheldon G Sheps, and Edward J Roccella. 2005. “Recommendations for Blood Pressure Measurement in Humans and Experimental Animals: Part 1: Blood Pressure Measurement in Humans: A Statement for Professionals from the Subcommittee of Professional and Public Education of the American Heart Association Cou.” *Hypertension* 45 (1): 142–61. doi:10.1161/01.HYP.0000150859.47929.8e.

48. Rao, P.Syamasundar, Haitham N Najjar, Mohammed K Mardini, Laszlo Solymar, and Mohinder K Thapar. 1988. “Balloon Angioplasty for Coarctation of the Aorta: Immediate and Long-Term Results.” *American Heart Journal* 115 (3): 657–65. doi:10.1016/0002-8703(88)90817-4.

49. Reichek, Nathaniel, and Richard B Devereux. 1982. “Reliable Estimation of Peak Left Ventricular Systolic Pressure by M-Mode Echographic-Determined End-Diastolic Relative Wall Thickness: Identification of Severe Valvular Aortic Stenosis in Adult Patients.” *American Heart Journal* 103 (2): 202–9. doi:10.1016/0002-8703(82)90493-8.

50. Richards, Dylan Jack, Yu Tan, Jia Jia, Hai Yao, and Ying Mei. 2013. “3D Printing for Tissue Engineering.” *Israel Journal of Chemistry*, September, n/a – n/a. doi:10.1002/ijch.201300086.

51. Riesenkampff, Eugénie, Urte Rietdorf, Ivo Wolf, Bernhard Schnackenburg, Peter Ewert, Michael Huebler, Vladimir Alexi-Meskishvili, et al. 2009. “The Practical Clinical Value of Three-Dimensional Models of Complex Congenitally Malformed Hearts.” *The Journal of Thoracic and Cardiovascular Surgery* 138 (3). Elsevier: 571–80. doi:10.1016/j.jtcvs.2009.03.011.

52. Rudolph, A M. 1979. “Fetal and Neonatal Pulmonary Circulation.” *Annual Review of Physiology* 41 (January). Annual Reviews 4139 El Camino Way, P.O. Box 10139, Palo Alto, CA 94303-0139, USA: 383–95. doi:10.1146/annurev.ph.41.030179.002123.

53. Sahn, David J., Hugh D. Allen, Stanley J. Goldberg, Robert Solinger, and Richard A. Meyer. 1975. “Pediatric Echocardiography: A Review of Its Clinical Utility.” *The Journal of Pediatrics* 87 (3): 335–52. doi:10.1016/S0022-3476(75)80633-0.

54. Salmi, Mika, Kaija-Stiina Paloheimo, Jukka Tuomi, Jan Wolff, and Antti Mäkitie. 2013. “Accuracy of Medical Models Made by Additive Manufacturing (rapid Manufacturing).” *Journal of Cranio-Maxillo-Facial Surgery : Official Publication of the European Association for Cranio-Maxillo-Facial Surgery* 41 (7): 603–9. doi:10.1016/j.jcms.2012.11.041.

55. Shaddy, R. E., A. R. Snider, N. H. Silverman, and W. Lutin. 1986. “Pulsed Doppler Findings in Patients with Coarctation of the Aorta.” *Circulation* 73 (1): 82–88. doi:10.1161/01.CIR.73.1.82.

56. Shahcheraghi, N., H. A. Dwyer, A. Y. Cheer, A. I. Barakat, and T. Rutaganira. 2002. “Unsteady and Three-Dimensional Simulation of Blood Flow in the Human Aortic Arch.” *Journal of Biomechanical Engineering* 124 (4). American Society of Mechanical Engineers: 378. doi:10.1115/1.1487357.

57. Sharland, G. K., K. Y. Chan, and L. D. Allan. 1994. “Coarctation of the Aorta: Difficulties in Prenatal Diagnosis.” *Heart* 71 (1): 70–75. doi:10.1136/hrt.71.1.70.

58. Sinclair, CM, and Manitoba. Provincial Court. 2000. “The Report of the Manitoba Pediatric Cardiac Surgery Inquest: An Inquiry into Twelve Deaths at the Winnipeg Health Sciences Centre in 1994.” https://scholar.google.co.uk/scholar?hl=en&as_sdt=0,5&q=manitoba+paediatric+cardiac+surgery+inquest#0.

59. Snider, A. R., and N. H. Silverman. 1981. “Suprasternal Notch Echocardiography: A Two-Dimensional Technique for Evaluating Congenital Heart Disease.” *Circulation* 63 (1): 165–73. doi:10.1161/01.CIR.63.1.165.

60. Stark, J, S Gallivan, J Lovegrove, JRL Hamilton, JL Monro, JCS Pollock, and KG Watterson. 2000. “Mortality Rates after Surgery for Congenital Heart Defects in Children and Surgeons’ Performance.” *The Lancet* 355 (9208): 1004–7. doi:10.1016/S0140-6736(00)90001-1.

61. Suárez de Lezo, José, Manuel Pan, Miguel Romero, Alfonso Medina, José Segura, Djordje Pavlovic, Carlos Martinez, et al. 1995. “Balloon-Expandable Stent Repair of Severe Coarctation of Aorta.” *American Heart Journal* 129 (5): 1002–8. doi:10.1016/0002-8703(95)90123-X.

62. Sun, Zhenxing, Tsung O Cheng, Ling Li, Li Zhang, Xinfang Wang, Nianguo Dong, Qing Lv, et al. 2015. “Diagnostic Value of Transthoracic Echocardiography in Patients with Coarctation of Aorta: The Chinese Experience in 53 Patients Studied between

2008 and 2012 in One Major Medical Center." *PloS One* 10 (6). Public Library of Science: e0127399. doi:10.1371/journal.pone.0127399.

63. Sweeney, Michael S., William E. Walker, J. Michael Duncan, Grady L. Hallman, James J. Livesay, and Denton A. Cooley. 1985. "Reoperation for Aortic Coarctation: Techniques, Results, and Indications for Various Approaches." *The Annals of Thoracic Surgery* 40 (1): 46–49. doi:10.1016/S0003-4975(10)61168-X.

64. Warnes, Carole A., Roberta G. Williams, Thomas M. Bashore, John S. Child, Heidi M. Connolly, Joseph A. Dearani, Pedro del Nido, et al. 2008. "ACC/AHA 2008 Guidelines for the Management of Adults With Congenital Heart Disease." *Journal of the American College of Cardiology* 52 (23). Journal of the American College of Cardiology: e143–263. doi:10.1016/j.jacc.2008.10.001.

65. Wood, N B, S J Weston, P J Kilner, A D Gosman, and D N Firmin. 2001. "Combined MR Imaging and CFD Simulation of Flow in the Human Descending Aorta." *Journal of Magnetic Resonance Imaging : JMRI* 13 (5): 699–713. http://www.ncbi.nlm.nih.gov/pubmed/11329191.

66. Wright, Gail E, Cheryl A Nowak, Caren S Goldberg, Richard G Ohye, Edward L Bove, and Albert P Rocchini. 2005. "Extended Resection and End-to-End Anastomosis for Aortic Coarctation in Infants: Results of a Tailored Surgical Approach." *The Annals of Thoracic Surgery* 80 (4). Elsevier: 1453–59. doi:10.1016/j.athoracsur.2005.04.002.

67. Zabal, C. 2003. "The Adult Patient with Native Coarctation of the Aorta: Balloon Angioplasty or Primary Stenting?" *Heart* 89 (1): 77–83. doi:10.1136/heart.89.1.77.

Appendix 1

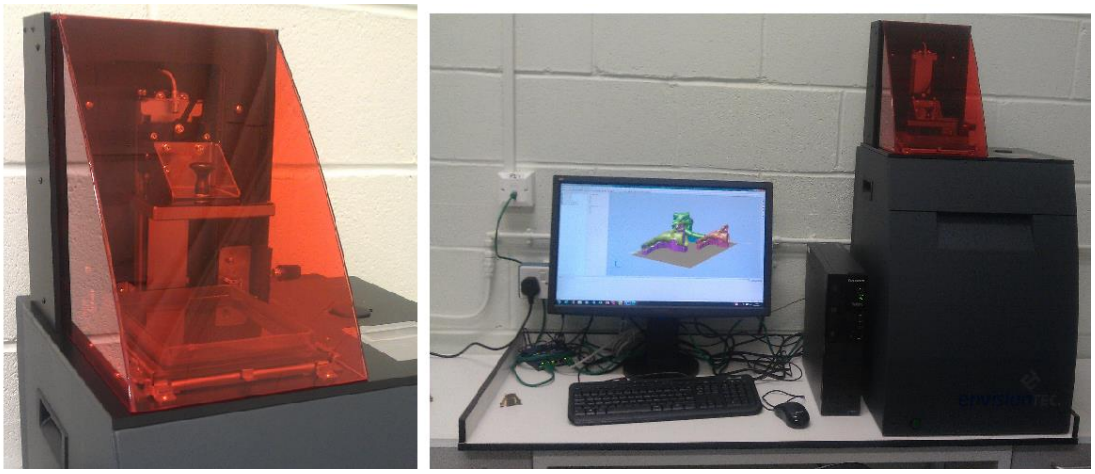

Fig 29. An image of the Perfactory® Desktop Digital Shell Printer by Envisiontech, the coloured glass covering the work area is to prevent UV light interacting with the resin.

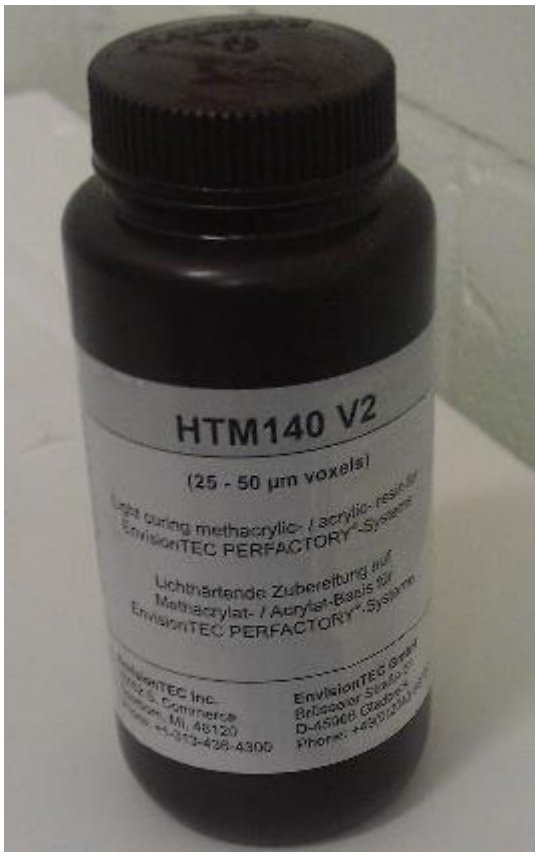

Fig. 30 showing the HTM 140 V2 resin used for printing.

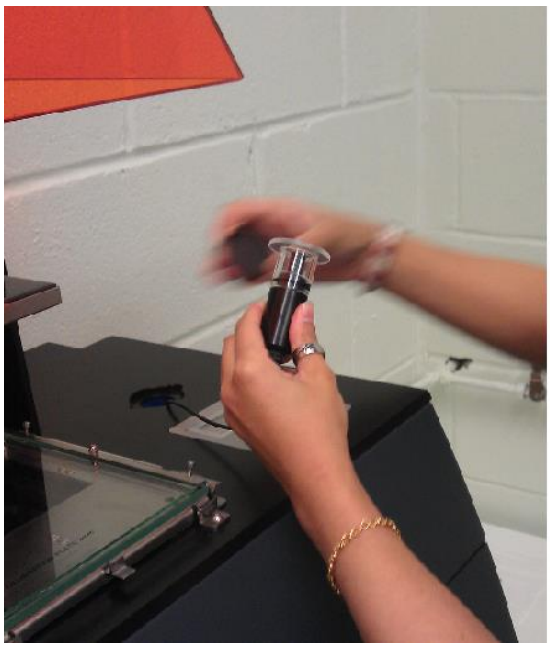
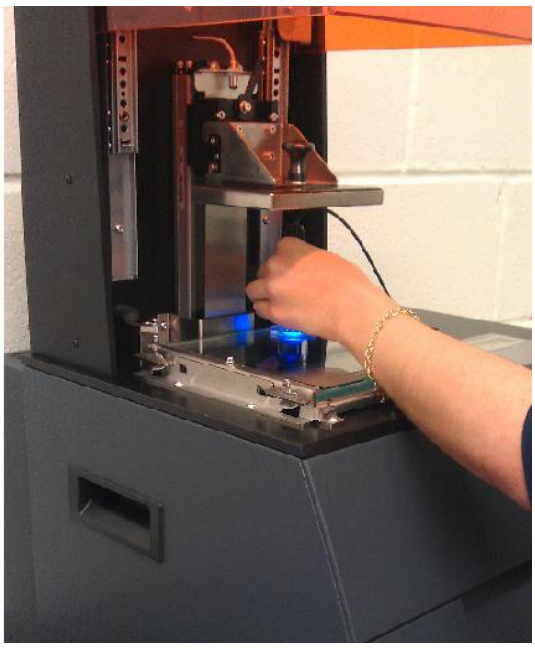

Fig. 31 showing the calibration process before each print. A probe is used to cover a light which is emitted at various points of the working area.

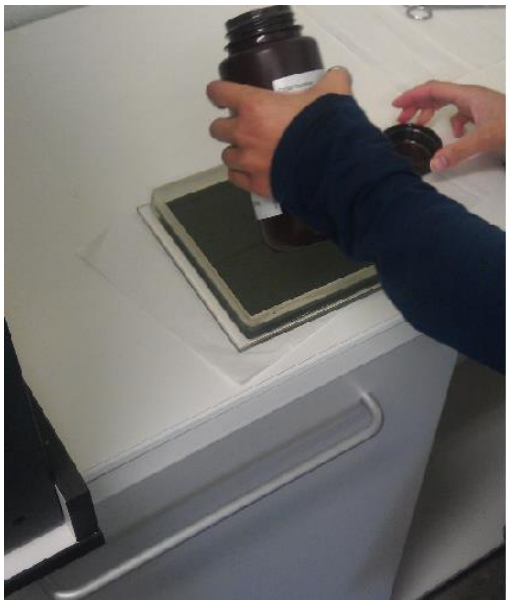
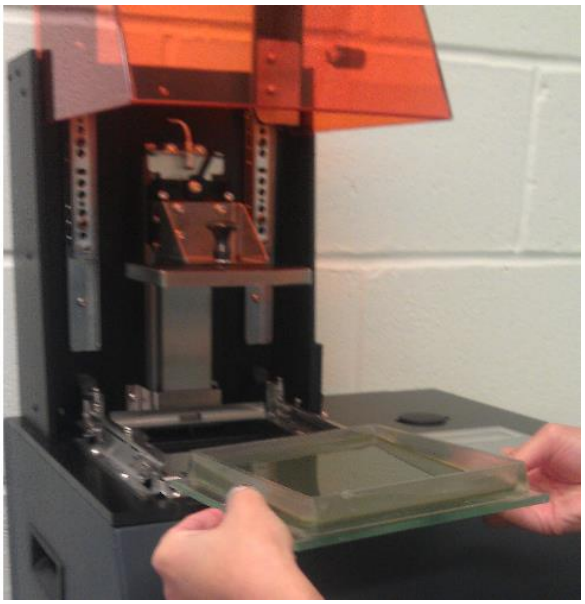

Fig. 32 showing the resin as it is being installed into the machine. From this pool of resin, the solid object will be synthesized using UV light. The object will emerge from the pool layer by layer.